MEASUREMENT OF CARBONATE CAPACITY OF HIGH TEMPERATURE POLYMERIC MELTS

By

KAMLESH KUMAR SINGH

DEPARTMENT OF METALLURGICAL ENGINEERING

INDIAN INSTITUTE OF TECHNOLOGY KANPUR

DECEMBER, 1992

MEASUREMENT OF CARBONATE CAPACITY OF HIGH TEMPERATURE POLYMERIC MELTS

A Thesis Submitted
in Partial Fulfilment of the Requirements
for the Degree of

MASTER OF TECHNOLOGY

By

KAMLESH KUMAR SINGH

to the

DEPARTMENT OF METALLURGICAL ENGINEERING
INDIAN INSTITUTE OF TECHNOLOGY KANPUR
DECEMBER, 1992

CERTIFICATE

This is to certify that the work **"Measurement of Carbonate Capacity of High Temperature Polymeric Melts"** has been carried out by Mr.Kamlesh Kumar Singh under my supervision and that it has not been submitted elsewhere for a degree.

A Ghosh

(A. Ghosh)
Professor
Department of Metallurgical Engineering
Indian Institute of Technology
KANPUR

ACKNOWLEDGEMENT

It is a great pleasure to express my deepest sense of gratitude and indebtedness to Professor A. Ghosh for suggesting the interesting problem, inspiring guidance, and valuable discussions and constant encouragement through out the course of this study.

I would like to express my hearty and sincere thanks to Mr.S.K. Choudhary, Mr.T.K. Roy, Mr.R.K. Goyal and Mr.S.K. Dutta for helping me during the experimental work as well as valuable suggestions rendered by them in the present study. I am thankful to Mr.A. Sharma for his valuable help and active cooperation during the entire period of this work.

I am also thankful to Mr. V. Sharma of ACMS for providing me some urgently needed chemicals for this work.

Thanks are also due to Mr.V.P. Vohra and Mr.R.C. Sharma of Metallurgical Engineering Workshop, for their help in the fabrication of silicon carbide rod furnace.

I express my sincere appreciation to Mr.B.D. Biswas for typing and Mr.V.P. Gupta for tracing of figures, and their sincere cooperation for timely completion of thesis.

I am thankful to family members of Professor A. Ghosh for providing me homelike environment during my stay in campus.

I express my heartfelt thanks to Pankaj and Sudipto for their help during my thesis work and to all my friends with whom I have had many days of pleasant association in the campus.

Finally I would like to offer my sincere thanks to my family members and relatives for their inspiration and encouragement in this study.

CONTENTS

LIST OF TABLES

LIST OF FIGURES

ABSTRACT

The basicity is a key parameter in connection with chemical properties of slags and other polymeric melts. Carbonate capacity of a slag is related to its basicity. In this investigation, measurements of CO_2 solubility of Na_2O-B_2O_3-SiO_2 melts were made by thermogravimetric method in the overall temperature range of 1000-1250^oC. The slags had mostly 50 mole pct. Na_2O, and varying B_2O_3 and SiO_2 contents from 0-50 mole pct.

The CO_2 solubility values obtained experimentally were within the ranges reported in literature for Na_2O-SiO_2 melt. The solubility of CO_2 decreased continuously with increasing B_2O_3 content in the melt and with increase in temperature at 50 mole pct. Na_2O. It shows that basicity of melt decreased with increase in B_2O_3 content at constant temperature. A linear dependence of logarithm of carbonate capacity with theoretical optical basicity was found for melts containing 50 mole pct. Na_2O. However the CO_2 solubility in 60 mole pct. Na_2O was much larger and did not match with the above line.

Determination of correct weight gain of melt due to absorption of CO_2 required correction for weight changes of sample due to upward drag force of flowing gas as well as loss of weight due to volatilization of components of slag. The rates of volatilization were determined from weight change vs. time curves. The rate increased significantly with increase of B_2O_3 content of slag. This is attributed to much larger vapour pressure of B_2O_3 as compared to that of Na_2O.

CHAPTER 1

INTRODUCTION

1.1 Objective

High temperature polymeric melts contain complex ions. In the context of high temperature technology, these refer to oxide melts containing acidic oxides such as silica, boric oxide, alumina, phosphorus oxide and may be classified as silicates, borates, borosilicates, alumino-silicates etc. In these melts cations such as Ca^{2+}, Na^{+} etc. are basically free, but anions are complex ones, such as $(SiO_4)^{4-}$, $(PO_4)^{3-}$ etc.

Technologically, polymeric melts may be classified as glass, slag, magma or flux depending on their application or occurrence. Slag is the collector of gangue and other impurities during extraction and refining of metals in liquid state at high temperature. Magma is molten rock coming out from interior of the Earth. Fluxes are used in joining of metals, for providing protection to the liquid metal or alloy during joining as well as to impart better properties to the joint. Electroslag welding processes employ large quantities of such fluxes/slags.

Other important uses of slags and fluxes are :

(i) as mould flux in continuous casting of steel,

(ii) in remelting of metals and alloys to obtain superior quality in special alloys by Electroslag remelting process,

(iii) for encapsulation of nuclear waste,

(iv) manufacture of cement from slag, and

(v) as fertilizer or soil conditioner.

It is important to control properties of these melts for technological applications for which they are meant. For this, choice of composition is crucial. One characteristic of these melts is that, properties such as viscosity, diffusivity and activity may vary by orders of magnitude in the same system and same temperature depending upon composition. In order to make them versatile addition of halides, such as CaF_2, $CaCl_2$, NaCl, is often taken recourse to.

In view of its importance, studies on structure and properties of these melts have been going on throughout the world. This is reflected by a series of International Conferences on molten slags and fluxes held in last 10 to 15 years. However, almost no study is going on in India to the best of author's knowledge. Therefore, it was decided to carry out some investigations. As the title of the thesis suggests, the study consisted of measurement of carbonate capacity of some melts. Carbonate capacity is related to basicity, which is a key parameter in connection with chemical properties of these melts.

1.2 Plan of Work

Keeping in mind the limitation of furnace temperature attainable in the laboratory it was decided to carry out measurements of carbonate capacity in B_2O_3 containing slags, which have low liquidus temperatures. Search of literature also showed relevance of these melts as slags, fluxes and glass. Moreover, not much measurements of carbonate capacity have been

made on them.

The slag systems were chosen as $CaO-B_2O_3-SiO_2$ with or without addition of CaF_2, and $Na_2O-B_2O_3-SiO_2$ with or without addition of CaO.

Measurement of carbonate capacity was carried out by equilibrating a slag sample in molten condition with carbon dioxide in a thermogravimetric set up and recording the weight gain due to absorption of carbon dioxide.

Program of the present study consisted of the following:

(i) literature review on slag basicity and capacities,

(ii) collection and pre-treatment of chemicals,

(iii) fabrication of slag melting set up,

(iv) choice of slag compositions,

(v) preparation of slags,

(vi) design of the hanging assembly for weight gain measurement by cahn automatic electrobalance,

(vii) measurement of carbon dioxide absorption at various slag compositions and temperatures,

(viii) processing of experimental data,

(ix) interpretation of results.

CHAPTER 2

LITERATURE REVIEW

2.1 Basicity of Slag

Basicity of a polymeric melt increases with increased percentage of basic oxides in it. Basicity of slag is an important parameter governing refining. Steelmakers had always been paying attention to it. Therefore the issue of basicity has been discussed and investigated in connection with slag only, so far as metallurgical engineering is concerned. Therefore, subsequently the terminology `slag' shall be used in the write up rather freely. It is to be emphasized again that the fundamentals are equally applicable to other polymeric melts as well.

Slags in which basic oxides (CaO,MgO,MnO,FeO,etc.) are predominant, are called basic slags and those with predominance of acidic oxides (SiO_2,P_2O_5,etc.) are termed acidic slags. An acidic oxide will absorb oxygen ions, when dissolved in a basic slag melt, and a basic oxide provides oxygen ions, when dissolved in a melt, as shown below.

$$SiO_2 + 2\ O^{2-} = SiO_4^{4-} \qquad \ldots(2.1)$$

$$CaO = Ca^{2+} + O^{2-} \qquad \ldots(2.2)$$

In industrial practices, the basicity is expressed as ratio of weight percentages of basic oxides to those of acidic oxides. An index of basicity commonly employed is the `Vee' ratio[1] where

$$V = \frac{\text{wt \% CaO}}{\text{wt \% } SiO_2} \qquad \ldots(2.3)$$

This ratio ignores the effect of other basic (FeO,MnO,MgO,etc.) and acidic (Fe_2O_3, Al_2O_3, P_2O_5, etc.) oxides, however it has been considered adequate as a basis for discussion of minor variations in a particular practice. Use of modified Vee ratio, based on the total contents of selected oxides in the slag, such as:

$$\frac{\text{wt \% CaO}}{\text{wt \% } SiO_2 + \text{wt \% } Al_2O_3} \quad \text{or} \quad \frac{\text{wt \% CaO}}{\text{wt \% } SiO_2 + \text{wt \% } P_2O_5}$$

have also been suggested.[2]

According to molecular model of slags, an alternative to the use of a basicity ratio is to make use of the concept of 'excess base'. In terms of molecular theory this will correspond to the amount of free oxide present after the requirement for basic oxides have been met, for the formation of stable neutral molecules. For example, if lime is considered to be the only important base, excess lime can be used as a basicity parameter. By assuming the formation of $2CaO.SiO_2$ and $3CaO.P_2O_5$, the excess base (B) may be expressed as[1]:

$$B = \text{wt \% CaO} - 1.86 \text{ wt \% } SiO_2 - 1.19 \text{ wt \% } P_2O_5 \qquad \ldots(2.4)$$

For a more complex slag, if the compounds $2MO.SiO_2$, $4MO.P_2O_5$, $2MO.Al_2O_3$, $MO.Fe_2O_3$ are assumed to exist undissociated in the slag, then in term of gram molecules the excess base $(B)^1$ is given as:

$$B = MO - 2SiO_2 - 4P_2O_5 - 2Al_2O_3 - Fe_2O_3 \qquad \ldots(2.5)$$

where MO represents a basic oxide.

In a basic slag melt, the anions are present as complex SiO_4^{4-}, PO_4^{3-}, AlO_3^{3-}, etc. as well as free O^{2-}, and free cations following the dissociation scheme :

$$w\ SiO_2 + x\ P_2O_5 + y\ Al_2O_3 + Z\ MO = w\ SiO_4^{4-} + 2x\ PO_4^{3-} + 2y\ AlO_3^{3-} + (z-2w-3x-3y)O^{2-} + ZM^{2+} \quad \ldots(2.6)$$

According to Lewis definition of acid and base, an acid is defined as any molecule, radical, or ion in which an atom, because of the presence of an incomplete electronic grouping, can accept one or more electron pairs (i.e. as electron pairs accepter). Correspondingly, a base is defined as a species that has within its molecular structure atom(s) that is (are) capable of donating electron pair(s) (i.e. as electron pairs donor).

According to the above definition, a basic oxide donates O^{2-} in a slag, whereas an acidic oxide absorbs O^{2-}. Since a basic oxide (e.g. CaO) tends to dissociate into cation and oxygen ion (e.g. Ca^{2+},O^{2-}), concentration of free O^{2-} increases with increasing basicity. From thermodynamic view point, activity of free oxygen ion in slag ($a_{O}2-$) may be taken as fundamental scientific index of basicity of slags. However its absolute value can not be determined. Even measurement of a relative value of $a_{O}2-$ is difficult. Hence,some other concepts have been evolved in the last two decades as measure of basicity of slags. One concept which is useful is that of `capacities' such as sulphide capacity, carbonate capacity etc. As will be shown later, the various capacities depend on activity of oxygen ion in slag.

However there are more parameters governing capacities. Hence, an important issue is how these can be related to basicity. Another concept is that of `optical basicity' of slag.

2.2 Sulphide Capacity of Slag

Sulphide capacity was defined by Richardson and Fincham[3] as `the potential capacity of a melt to hold sulphur as sulphide'. They denoted it by C_s and mathematically defined as

$$C_s = (\text{wt \% } S^{2-}) \left[\frac{P_{O_2}}{S_2}\right]^{1/2} \qquad ...(2.7)$$

At low p_{O_2} (less than 10^{-5} atmosphere for steelmaking) the sulphur is present in the slag primarily as sulphide. For gas-slag reaction, its concentration would be controlled by the equilibrium of the reaction.

$$\frac{1}{2} S_2(g) + (O^{2-}) = \frac{1}{2} O_2(g) + (S^{2-}) \qquad ...(2.8)$$

The equilibrium relation for the reaction (2.8) may be written as

$$K_8 = \frac{a_{S^{2-}}}{a_{O^{2-}}} \cdot \left(\frac{P_{O_2}}{P_{S_2}}\right)^{1/2} = \frac{(\text{wt \% } S^{2-}) \cdot f_{S^{2-}}}{a_{O^{2-}}} \left(\frac{P_{O_2}}{P_{S_2}}\right)^{1/2} \qquad ...(2.9)$$

$$\text{or} \quad C_s = (\text{wt \% } S^{2-}) \left(\frac{P_{O_2}}{P_{S_2}}\right)^{1/2} = \frac{K_8 \cdot a_{O^{2-}}}{f_{S^{2-}}} \qquad ...(2.10)$$

where, p_{O_2} = partial pressure of oxygen in gas

p_{S_2} = partial pressure of sulphur in gas

$a_{O^{2-}}$ = activity of oxygen ion in slag

f_S^{2-} = activity coefficient of sulphide ion in slag

K_8 = equilibrium constant of reaction (2.8).

C_s is a property of a slag, and it depends only on the composition of the slag and temperature. Hence measured values of sulphide capacity of slags have been compiled in books and can be used by others. The greater is the C_s value, higher is the extent of sulphur absorption by the slag. There have been many measurements of sulphide capacities of slags. Few recent studies done by various investigators[4-5] for different slag systems at different temperatures may be referred.

2.3 Carbonate and Other Capacities of Slag

The carbonate capacity was proposed as a measure of basicity of slag by Wagner[6] on the basis of some scattered studies by physical chemists. It represents ability of a slag to absorb CO_2 from gas phase. Qualitatively speaking, more basic the slag is, more CO_2 it would absorb. It was defined on the basis of following gas-slag reaction:

$$CO_2(g) + (O^{2-}) = (CO_3^{2-}) \qquad ...(2.11)$$

The equilibrium constant of the reaction may be written as:

$$K_{11} = \frac{a_{CO_3^{2-}}}{P_{CO_2} \cdot a_{O^{2-}}} = \frac{(\text{ wt \% } CO_3^{2-}) \cdot f_{CO_2}}{P_{CO_2} \cdot a_{O^{2-}}}$$

$$C_c = \frac{(\text{ wt \% } CO_3^{2-})}{P_{CO_2}} = \frac{K_{11} \cdot a_{O^{2-}}}{f_{CO_3^{2-}}} \qquad ...(2.12)$$

where, C_c = carbonate capacity of slag; it is a property

of slag like C_s

P_{CO_2} = partial pressure of CO_2 in gas

$a_{CO_3^{2-}}$ = activity of carbonate ion in slag

$f_{CO_3^{2-}}$ = activity coefficient of CO_3^{2-} in slag

$a_{O^{2-}}$ = activity of oxygen ion in slag.

Similar to the C_c, Wagner[6] also defined the phosphate capacity (C_p) on the basis of following reaction.

$$\frac{1}{2} P_2(g) + \frac{5}{4} O_2(g) + \frac{3}{2} (O^{2-}) = (PO_4^{3-}) \quad \ldots(2.13)$$

The equilibrium relation for this reaction may be written as

$$K_{13} = \frac{1}{(p_{P_2})^{1/2} (p_{O_2})^{5/4}} \cdot \frac{a_{PO_4^{3-}}}{(a_{O^{2-}})^{3/2}}$$

$$= \frac{1}{(p_{P_2})^{1/2} (p_{O_2})^{5/4}} \cdot \frac{(\text{wt \% } PO_4^{3-}) \cdot f_{PO_4^{3-}}}{(a_{O^{2-}})^{3/2}} \quad \ldots(2.14)$$

$$\text{or, } C_P = (\text{wt \% } PO_4^{3-}) / \left(p_{P_2}^{1/2} \cdot p_{O_2}^{5/4}\right) = \frac{K_{13} \cdot (a_{O^{2-}})^{3/2}}{f_{PO_4^{3-}}} \quad \ldots(2.15)$$

If the concentrations of CO_3^{2-}, PO_4^{3-} and S^{2-} ions are low, then according to Henry's law, activity coefficients have constant values independent of composition. Hence it may be assumed that $fCO_3^{2-} = f^o CO_3^{2-}$, $fS^{2-} = f^o S^{2-}$ and $f PO_4^{3-} = f^o PO_4^{3-}$. Then equations (2.10), (2.12) and (2.15) may be written as

follows:

$$C_s = (\text{wt \% } S^{2-})\ (p_{O_2} / p_{S_2})^{1/2} = \frac{K_8 \cdot a_{O^{2-}}}{f^o_{S^{2-}}} \qquad \ldots(2.16)$$

$$C_c = \frac{(\text{wt \% } CO_3^{2-})}{p_{CO_2}} = K_{11} \frac{a_{O^{2-}}}{f^o_{CO_3^{2-}}} \qquad \ldots(2.17)$$

and $$C_P = (\text{wt \% } PO_4^{3-}) \Big/ \left(p_{P_2}^{1/2} \cdot p_{O_2}^{5/4}\right) = \frac{K_{13} \cdot (a_{O^{2-}})^{3/2}}{f^o_{PO_4^{3-}}} \qquad \ldots(2.18)$$

From equations (2.16), (2.17) and (2.18) one may write

$$\frac{C_s}{C_c} = \frac{f^o_{CO_3^{2-}}}{f^o_{S^{2-}}} \cdot \frac{K_8}{K_{11}} \qquad \ldots(2.19)$$

and $$\frac{C_P}{(C_c)^{3/2}} = \frac{(f^o_{CO_3^{2-}})^{3/2}}{f^o_{PO_4^{3-}}} \frac{K_{13}}{(K_{11})^{3/2}} \qquad \ldots(2.20)$$

$$\frac{C_P}{(C_s)^{3/2}} = \frac{(f^o_{S^{2-}})^{3/2}}{(f^o_{PO_4^{3-}})} \cdot \frac{K_{13}}{(K_8)^{3/2}} \qquad \ldots(2.21)$$

Wagner[6] proposed that as a tentative working hypothesis, one may assume that the quotients on the right hand side of equations (2.19), (2.20) and (2.21) depend on the concentration of the majority component of slag only to a minor extent. Thus, using activity coefficients in a suitable reference slag (marked by an asterisk superscript), one obtains from equations (2.19), (2.20) and (2.21).

$$\frac{C_s^{o*}}{C_c} = \frac{f_{CO_3^{2-}}}{f^{o*}_{S^{2-}}} \cdot \frac{K_8}{K_{11}} \qquad \ldots(2.22)$$

$$\frac{C_p}{(C_c)^{3/2}} = \frac{(f^{o*}_{CO_3^{2-}})^{3/2}}{f^{o*}_{PO_4^{3-}}} \cdot \frac{K_{13}}{(K_{11})^{3/2}} \qquad \ldots(2.23)$$

$$\frac{C_p}{(C_s)^{3/2}} = \frac{(f^{o*}_{S^{2-}})^{3/2}}{f^{o*}_{PO_4^{3-}}} \cdot \frac{K_{13}}{(K_8)^{3/2}} \qquad \ldots(2.24)$$

where, the right hand terms are constants i.e. independent of slag composition.

If the quotients on the left hand side of equations (2.22), (2.23) and (2.24) are approximately independent of the mole fractions of the majority components of slags used for particular slag system, then upon comparing capacities of species `i' and `j' in different slags denoted by prime and double prime superscripts, one obtains

$$\left(\frac{C''_j}{C'_j}\right)^{1/V_j} = \left(\frac{C''_i}{C'_i}\right)^{1/V_i} \qquad \ldots(2.25)$$

where V_i and V_j are the numbers of O^{2-} ions involved in reactions (2.8), (2.11) and (2.13). Thus if the capacities C'_i and C''_i of species `i' in two slags of different composition have been determined, one may predict approximately the ratio of the capacities $C''_j$ and $C'_j$ of species `j' in these slags. Hence it is natural that the various capacities are inter-related. An example is presented in Fig.2.1[7], which shows log C_p vs. log C_s in various slag systems. It can be shown from equation (2.21) that

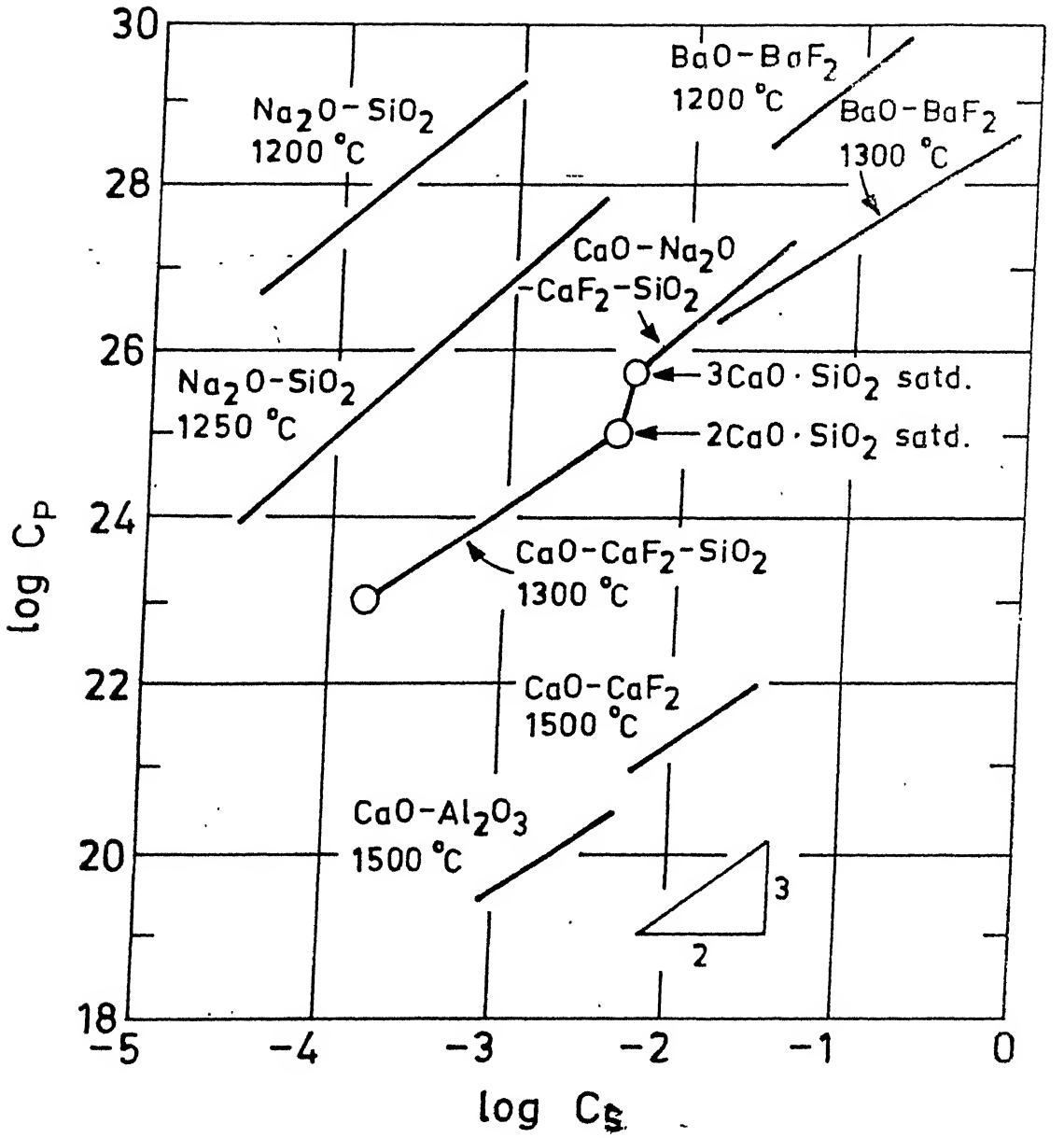

Fig. 2.1. Relationship between sulphide capacities and phosphate capacities for various basic fluxes[7]

$$\log C_p = 3/2 \log C_s + \log K_{26} \cdot \frac{(f^o_{S^{2-}})^{3/2}}{f^o_{PO_4^{3-}}}$$

...(2.26)

$K_{26} = \frac{K_{13}}{(K_8)^{3/2}}$, is an equilibrium constant term and depends only on temperature.

At constant temperature, in the same slag system (e.g. Na_2O-SiO_2 system), $(f^o_{S^{2-}})^{3/2}/f^o_{PO_4^{3-}}$ parameter is expected to be constant[6]. Hence a single straight line with slope of 3/2 is expected. Fig.2.1 agrees with this analysis. Of course, a corollary to this conclusion is that there is no Universal correlation between $\log C_p$ vs. $\log C_s$ which will be applicable to all kinds of slag system. Similar conclusion can be drawn about inter-relationships of other capacities.

Considerable interest has been evinced in recent years on the possibility of lowering of nitrogen content of liquid steel by synthetic slag treatment. This requires use of a slag with high nitride capacity. It has been concluded by some investigators[8-10] that in a basic melt, nitrogen dissolves in slag as N^{3-} according to the reaction

$$1/2\ N_2(g) + 3/2\ (O^{2-}) = (N^{3-}) + \frac{3}{4}\ O_2(g)$$

...(2.27

As an analogy to other slag capacities, nitride capacity was defined as

$$C_{N^{3-}} = (\text{wt \% } N^{3-})\ P_{O_2}^{3/4} / P_{N_2}^{1/2} = \frac{K_{27} \cdot (a_{O^{2-}})^{3/2}}{f_{N^{3-}}}$$

...(2.28)

based on the ionic gas-slag reaction expressed by reaction (2.27). Here K_{27}, a_O^{2-} and f_N^{3-} are the equilibrium constant of equation (2.27), oxygen ion activity, and the activity coefficient of nitride ion, respectively. Nitride capacity increases steadily with SiO_2 and Al_2O_3 content of slag (Fig.2.2)[10]. This is due to stabilities of Si_3N_4 and AlN at high temperatures.

Furthermore Wagner[6] defined the basicity of a slag of arbitrary composition with the carbonate capacity C_c by

$$B_{Car} = C_c / C_c^* \qquad ...(2.29)$$

where, C_c^* is the carbonate capacity in a reference slag (e.g. 0.4 CaO + 0.4 SiO_2 + 0.2 Al_2O_3) which is liquid above 1300°C[11].

From equation (2.25) and (2.29) it follows that for the capacity of species `j'

$$C_j = C_j^* B_{Carb}^{V_j} \qquad ...(2.30)$$

In view of equation (2.25), one may also use the capacity of a species other than CO_3^{2-} for the definition of basicity e.g.

$$B_{Sulf} = C_S / C_S^* \qquad ...(2.31)$$

where B_{Sulf} is nearly but not exactly equal to B_{Carb} according to Wagner[6]. Hence use of C_c for definition of basicity, B, according to equation (2.29), was recommended by Wagner[6], since according to him changes of the activity coefficients of other solutes with slag composition are probably greater than changes of $f_{CO_3^{2-}}$. This was ascribed to greater interaction of ions like S^{2-} with cations than that of CO_3^{2-} with cations.

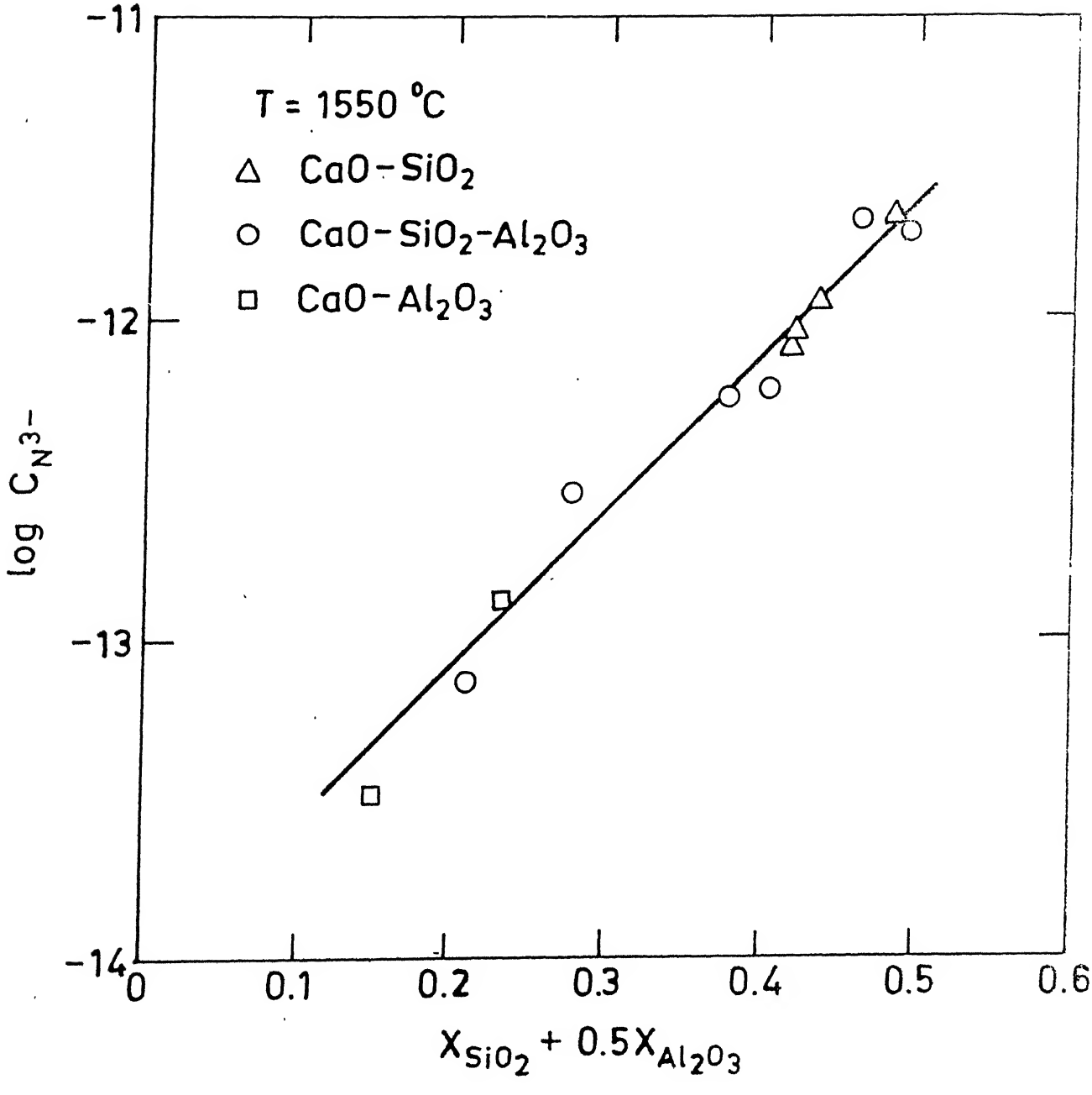

Fig. 2.2. Logarithm of nitride capacity versus $(X_{SiO_2} + 0.5\ X_{Al_2O_3})$ in slag[10]

Equation (2.30) provides a method to calculate other capacities in a slag by knowing the B_{Carb}. Experimental measurement of carbonate capacity on the basis of equation (2.12) is reasonably easy. Hence this approach attracted attention of other investigators. There have been several measurements of carbonate capacities of slags and attempts for correlation with basicity etc. These will be presented in detail later.

2.4 Optical Basicity of Slag

Optical basicity concept was developed in the field of glass chemistry[12-13] and it expresses the basicity in terms of the electron donor power of the oxide ions in glass. Commercially important glasses consist essentially of metal silicates, often with small quantities of phosphate, borate and other anions.

Duffy and Ingram[12] stated that the ability of oxygen to donate negative charge is at a maximum, when it exists as free O^{2-} ion, not influenced by surrounding cations. This situation is approached when the cations are almost non-polarizing. Certain metal ions undergo observable changes (e.g. a colour change due to a change of oxidation state) depending upon the electron donation they receive from the oxygen, and therefore they may be used as `probes' for basicity in glasses. The probe ions which respond in this way are p-block metal ions in oxidation state two units less than the number of the group to which they belong e.g. Ti^{+} (group III), Pb^{2+} (group IV) and Bi^{3+} (group V), and which have an electronic configuration $d^{10}\ s^{2}$. When small quantities of these probe ions are dissolved in glass, the electron donation by

the oxygen to the probe ion brings about a reduction in the 6S-6P energy gap, and this in turn produces a shift in frequency in the ultraviolet (UV) band as compared to that of the free probe ion. This effect can be measured spectroscopically in transparent glasses and slags. The technique is difficult to apply to steelmaking slags, since these are generally opaque.

Basic oxides are highly electron donating: Calcium oxide (CaO) has been chosen as a reference material for expressing the electron donor power of materials composed of acidic or basic oxides such as slags or glasses, and for these media, the ratio

$$\frac{\text{electron donor power of medium}}{\text{electron donor power of CaO}}$$

has been called the optical basicity. Using Pb^{2+} (most popular) as probe ion, the optical basicity (Λ) is given by

$$\Lambda = \frac{V_{free} - V_{sample}}{V_{free} - V_{CaO}} = \frac{60700 - V_{sample}}{31000} \qquad \ldots(2.32)$$

where V_{free}, V_{CaO} and V_{sample} are the peak wave numbers of s-p spectra of Pb^{2+} in the free state, in CaO and in the sample respectively.

When the probe ion is influenced by the less basic oxides of a glass, the frequency shift is less. For example in $CaO-P_2O_5$ (1:1) glass, the frequency of Pb^{2+} is 46200 cm^{-1} while in Na_2O-SiO_2 (3:7) glass, it is 42200 cm^{-1}, corresponding to shifts of 14500 and 18500 cm^{-1} respectively. The spectroscopic shift is a measure of the electron donor power of the glass.

From a large number of measurements on glasses using Pb^{2+} as the probe ion, it has been established that the optical basicity (Λ_i) of an oxide (i) is related to the Pauling electronegativity (α_i) of the cation by Duffy et al[13] as

$$\Lambda_i = 1/1.36\ (\alpha_i - 0.26) \qquad \ldots(2.33)$$

The electronegativity of an atom in a compound is the tendency to attract the shared pair of electrons towards itself. Alkali metals are least electronegative and hence their oxides have higher optical basicity. From equation (2.33), it is possible to calculate the optical basicity for any non-transitional metal oxide. The optical basicity calculated from the electronegativity value using equation (2.33) is called the theoretical optical basicity (Λ_{th}).

The Λ_{th} of slags containing multiple oxides can be calculated[14] by using the equation

$$\Lambda_{th} = \Sigma X_i\ \Lambda_{th,i} \qquad \ldots(2.34)$$

where X_i = The equivalent cation fraction of oxide (i)

$$\text{in slag/glass} = \frac{\text{Ni} \times \text{Number of oxygen atoms in (i)}}{\Sigma(\text{Ni} \times \text{Number of oxygen atoms in (i)})} \qquad \ldots(2.35)$$

$$\text{where Ni = Mole fraction of oxide (i)} = \frac{\text{wt \% (i)} / \text{M (i)}}{\Sigma\ \text{wt \% (i)} / \text{M (i)}} \qquad \ldots(2.36)$$

Another way to express the theoretical optical basicity is[15]:

$$\Lambda_{th} = \frac{X_A}{\gamma_A} + \frac{X_B}{\gamma_B} + \ldots \qquad \ldots(2.37)$$

where X_A, X_B are the equivalent cation fraction of oxides and γ_A,

γ_B are the 'basicity moderating parameters' of respective oxides. The basicity moderating parameter (γ) is the ability of the cations to use the oxide (-II)[15] charge clouds for covalency.

On the basis of equation (2.34), theoretical optical basicity for any system comprised of various oxides (in the mole ratio, $N_A : N_B :.....$) can be calculated[16] by considering the proportion of oxygen atom in each compound and its individual optical basicity values [$\Lambda(A_xO_a)$, $\Lambda(B_xO_b)$.....] as follows.

$$\Lambda = \frac{1}{(a\ N_A + b\ N_B + \ldots)} [a\ N_A\ \Lambda(A_xO_a) + b\ N_B\ \Lambda(B_xO_b) + \ldots] \quad \ldots(2.38)$$

The usual formulation of oxides A_xO_a, B_xO_b .... (which takes account of odd oxidation numbers $+a_1$, $+b_1$.... by making x = 2 but otherwise x = 1). If they are formulated normalised to a single cation, for example, Al_2O_3 as $AlO_{3/2}$, then it might be necessary to change the $N_A : N_B :....$ ratio.

In order to calculate the theoretical optical basicity of a system composed of fluorides CF_c, DF_d, ..., the formula analogous to equation (2.38) has been employed[16]

$$\Lambda = \frac{1}{(c\ N_C + d\ N_D + \ldots)} [c\ N_c\ \Lambda(CF_c) + d\ N_d\ \Lambda(DF_d) + \ldots.] \quad \ldots(2.39)$$

For mixed oxide-fluoride system, it is[16]

$$\Lambda = \frac{[a\ N_A\ \Lambda(A_xO_a) + b\ N_B\ \Lambda(B_xO_b) + \ldots + c\ N_C\ \Lambda(CF_c) + d\ N_D\ \Lambda(DF_d) + .]}{(a\ N_A + b\ N_B + \ldots\ldots + c\ N_C + d\ N_D + \ldots\ldots)} \quad \ldots(2.40)$$

Equation (2.37) for oxide system may be written in an alternate form as[13]:

$$\Lambda = \frac{Z_A r_A}{2} \cdot \frac{1}{\gamma_A} + \frac{Z_B r_B}{2} \cdot \frac{1}{\gamma_B} + \ldots \quad \ldots(2.41)$$

where Z_A, Z_B, ... are the oxidation numbers of cations and r_A, r_B , ... are the ratio of the cations with respect to the total number of oxygen atoms in the oxides. In Na_2O-P_2O_5 (1:1) glass, $r_{Na} = \frac{1}{3}$, $r_P = \frac{1}{3}$ and $Z_{Na} = 1$, $Z_P = 5$. Hence for this glass Λ = 0.525 from equation (2.41). Similarly for the glass Na_2O-SiO_2 (3:7), the $r_{Na} = \frac{6}{17}$, $r_{Si} = \frac{7}{17}$ and $Z_{Si} = 4$. Hence for this glass, Λ = 0.597 from equation (2.41).

The basicity moderating parameters (γ_i) for some elements are presented in Table (2.1). These were calculated from their Pauling electronegativity values (α_i) by using following equation[13]

$$\gamma_i = 1.36\ (\alpha_i - 0.26) \quad \ldots(2.42)$$

Table (2.2) presents optical basicities of different oxides. It has been taken largely from compilation by Bergman and Gustafsson[20]. Present author has also cross-checked these values from the original papers (18,21-23) from which these have been collected. Fig.2.3[13] shows agreement between Λ_{th} and experimental optical basicity values. It also shows that the optical basicity is medium independent and hence it may be applied to slag systems. Duffy et al[17] applied the optical basicity concept to metallurgical slags for the first time.

Since Λ is taken as 1 for CaO, the optical basicity in the context of slag chemistry can be visualized as an expression of 'lime character'[17]. The distinctive feature of this concept is that lime character values can be assigned even to slags that

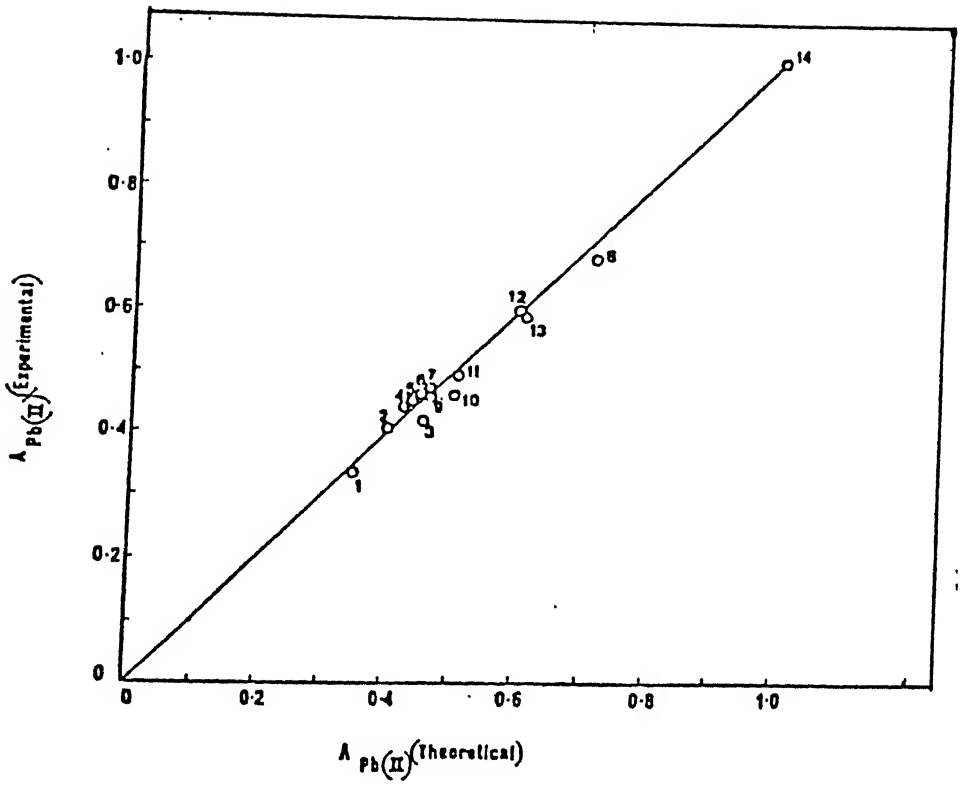

Fig. 2.3. Theoretical optical basicity versus experimental optical basicity[13]

[(1)100% H_2SO_4 (2)100% H_3PO_4 (3)$NaHSO_4$-$KHSO_4$ (1:1) glass (4)B_2O_3 glass (5)-(8) Na_2O-B_2O_3 glasses containing (5)5% (6)10% (7)15% (8)67% Na_2O (9)K_2SO_4-$ZnSO_4$ glass (10)$Ca_3(PO_4)_2$ (11)K_2O-Al_2O_3-B_2O_3 (15.4:15.4:69.2) (12) Al_2O_3 (13)Na_2O-SiO_2 (3:7) (14)CaO]

Table 2.1 : Values of γ for some elements[13]

Elements	γ	Elements	γ
Chlorine	3.73	Aluminium	1.65
Nitrogen	3.73	Magnesium	1.28
Sulphur	3.04	Calcium	1.00
Carbon	3.04	Lithium	1.00
Phosphorus	2.50	Sodium	0.87
Hydrogen	2.50	Potassium	0.73
Boron	2.36	Rubidium	0.73
Silicon	2.09	Cesium	0.60
Zinc	1.85		

contain no calcium oxide. Sosinsky et al[21] extended a previous correlation[17] between the sulphide capacity and optical basicity of slags by the addition of a considerable amount of fresh data[24]. The resulting relationship as shown in Fig.2.4 at a temperature of 1500°C, is

$$\log C_S = 12.6\,\Lambda - 12.3 \qquad \ldots(2.43)$$

Sosinsky et al[21] further extended equation (2.43) to any temperature in the range 1400°C to 1700°C as

$$\log C_S = \left(\frac{22690 - 54640\Lambda}{T}\right) + 43.6\,\Lambda - 25.2 \qquad \ldots(2.44)$$

Bergman et al[20] employed all the 3 sets of Λ values for correlation with monomer phosphorus capacity (CPM) for a variety of slags at 1600°C. The CPM is defined as:

$$CPM = \frac{(\%\ P_M)}{[\%\ P]\ [\%\ O]^{5/2}} = \frac{L_{PM}}{[\%\ O]^{5/2}} \qquad \ldots(2.45$$

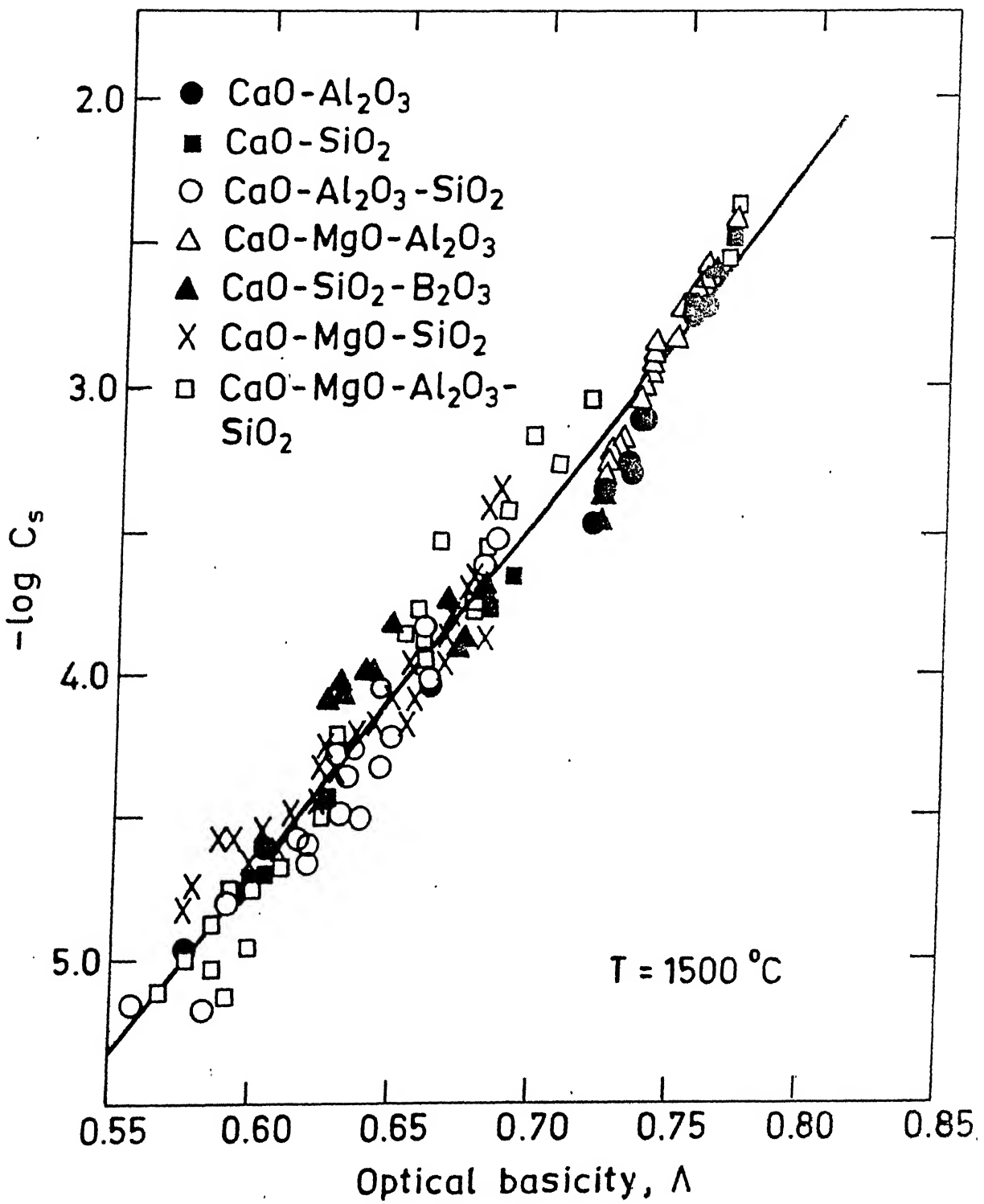

Fig. 2.4. Logarithm of sulphide capacity versus optical basicity

Table 2.2 : Comparison of different scale of optical basicity[20]

Oxides	Theoretical from Pauling electro-negativity[26]	Sosinsky & Sommerville[21] from sulphide capacity	Nakamura et al[18] from electron-density
K_2O	1.40		1.16
Na_2O	1.15	1.33[19]	1.11
BaO	1.15		1.08
Li_2O	1.00		1.06
CaO	1.00		1.00
MgO	0.78		0.92
TiO_2	0.61	0.61	0.65
Al_2O_3	0.605		0.66
MnO	0.59	1.21	0.95
ZnO	0.55		-
FeO	0.51	1.03	0.94
Fe_2O_3	0.48	0.70	0.72
SiO_2	0.48		0.47
B_2O_3	0.42		0.42
P_2O_5	0.40		0.38
H_2O	0.40		-
SO_3	0.33		0.29
CO_2	0.33		-

where, $L_{PM} = \frac{(\%\ P_M)}{[\%\ P]}$ = Equilibrium distribution

Coefficient of phosphorus between slag and steel.

$(\%\ P_M)$ = wt % of Monomer phosphate ion in slag

[% P] = wt % of Phosphorus in steel

[% O] = wt % of Oxygen in steel.

The correlation is presented in Fig.2.5. It may be noted that only theoretical optical basicity estimated by equation (2.33) yielded a systematic correlation of optical basicity with other parameters, even for slags containing some transition metal oxides.

2.5 Concluding Remarks on Optical Basicity of Slag

Sosinsky et al[21] estimated Λ from C_S for transition metal oxides (MnO,FeO,Fe_2O_3 and TiO_2). However these are widely different from Λ calculated theoretically from Pauling electronegativity (Table 2.2). It may also be noted from Table 2.2 that estimations of Λ from electron density by Nakamura et al[18] do not normally agree with theoretical optical basicity from Pauling electronegativties.

Experimental measurements of Λ are made on thin sections of samples of the solidified glass, and can be made only in the absence of any transition metal oxides, which render the glass opaque[21]. Such a technique is not applicable to metallurgical slags which normally contain at least small amount of transition metal oxides such as ferrous or manganese oxide. Equation (2.33) is an empirical equation based on data in aqueous solution and some glasses. This shows that it is perhaps medium-independent and should be applicable to slag. But can it be justified theoretically? A related observation is that Λ for Na_2O on the basis of Equation (2.33) is 1.15. However Gaskell[19], through an elaborate analysis of relation of Λ with $\gamma_{P_2O_5}$ and C_S in slag, has suggested that it should be taken as 1.33. In addition, assignment of correct value of Λ_{th} to transition metal

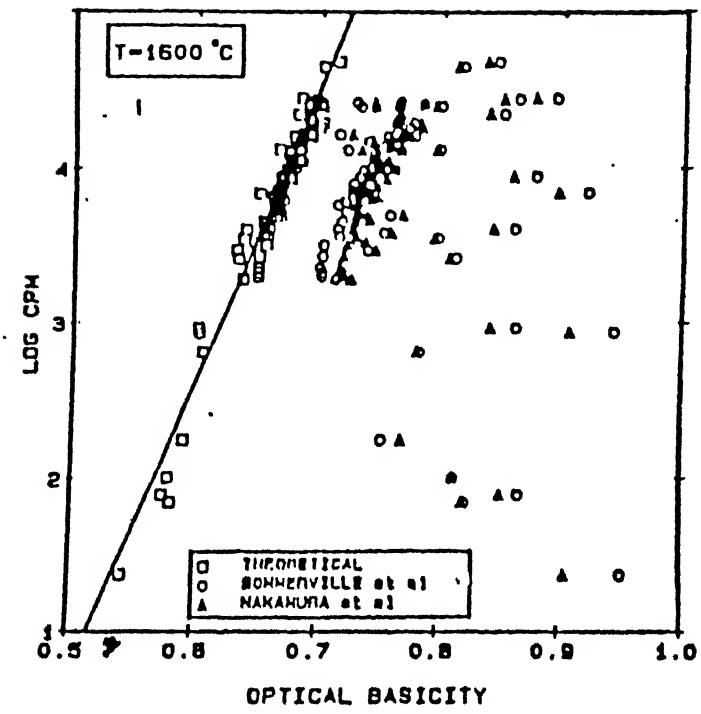

Fig. 2.5. Relationship between the logarithm of the monomer phosphorus capacity and the three scales of basicity[20]

oxides such as iron oxide, manganese oxide is still controversial, since equation (2.33) is not applicable for these from theoretical consideration.

There are some papers in the 3rd International Conference on molten slags and fluxes which have dealt with some of these. Duffy[15] has suggested an alternative method of measuring optical basicity of opaque materials using refractivity of divalent oxide. Ingram[25] has concluded that probably an invariant λ value (i.e. Λ-value) can not be assigned to the transition metal oxides. It would depend on the purpose for which it is being used, e.g. for reaction of sulphur or phosphorus or something else. Yokokawa and Mackawa[26] have tried to estimate electron donating power of oxides (which determines optical basicity) from X-Ray energy shifts, radiation-induced visible absorption spectroscopy, and quantum mechanical calculations.

2.6 Measurement of Carbonate Capacity and its Correlation with Other Quantities

The composition of slags and fluxes is complex and it is not correct to express the basicity of various slags and fluxes by a simple ratio of basic oxides and acidic oxides like $(CaO)/(SiO_2)$. There are problems of measurement or estimation of optical basicity of slags, since these mostly contain transition metal oxides. Therefore another index is necessary for basicities of various slags that can be determined reasonably easily by experiments. The concept of carbonate capacity (C_c) was found to be convenient as a measure of basicity by Wagner[6]. It has been

described earlier.

Table 2.3 presents the studies reported in literature on different slag systems at various temperature ranges by few investigators. It also shows the techniques employed for determination of carbonate capacities.

Maeda et al[27] studied the carbon dioxide solubilities in Na_2O-SiO_2 melts over the composition range X_{Na_2O} / (X_{Na_2O} + X_{SiO_2}) = 0.5 to 1.0, and temperature range of 1100°C to 1300°C. Fig.(2.6) and Fig.(2.7) show[26] that solubility of CO_2 increases with increasing X_{Na_2O} and decreases with increasing temperature respectively. Fig.(2.8)[27] compares the carbonate capacity from the experimental results with the values of sulphide and phosphate capacities obtained from the literature. In addition Maeda et al[27] also obtained a good correlation between carbonate capacity and activity of sodium oxide, which is shown in Fig.(2.9).

Sosinsky et al[28] measured the carbonate capacity in the CaO-Al_2O_3-SiO_2 system at temperatures between 1525°C and 1600°C by thermogravimetric method. They obtained a linear correlation between C_C and Λ. In this slag system, C_C displayed a positive temperature coefficient, so that the two effects of composition and temperature could be incorporated into a composite expression.

$$\log C_C = \left(\frac{100772 - 142645\Lambda}{T}\right) + 93.75\Lambda - 64.96 \qquad ...(2.46)$$

Sosinsky et al[28] claimed that, from this expression C_C could be calculated for a wide range of composition and temperature of interest for steelmaking and post furnace treatment prior to

Table 2.3 : Studies on Carbonate Capacity of Slag

Investigators Year and Reference	System Studied	Temp.Range, ^oC	Measurements	
			Quantity Determined	Technique
Ikeda et al[31] (1990)	$CaO-CaF_2-SiO_2$	1200-1500	Carbonate capacity	Thermogravimetry
Maeda et al[32] (1990)	$CaO-CaCl_2-CaF_2$	900-1500	CO_2 solubility	Thermogravimetry
Maeda et al[27] (1990)	Na_2O-SiO_2	1100-1300	CO_2 solubility	Gravimetric and chemical analyses
Kawahara et al[29] (1986)	Highly basic melt	1200-1500	CO_2solubility	Gravimetric and chemical analyses
Karvonen et al[30] (1988)	SiO_2-Na_2O-XO (X=Li_2,Ba,SrCa)	1100-1250	Carbonate capacity	Thermogravimetry
Sosinsky et al[28] (1986)	$CaO-Al_2O_3-SiO_2$	1525-1600	Carbonate capacity	Thermogravimetry
Kawahara et al[33] (1986)	$BaO-BaF_2$ Na_2O-SiO_2 $Na_2O-PO_{2.5}$ $Na_2O-SiO_2-FeO-FeO_{1.5}$ $CaO-Al_2O_3$. $CaO-CaF_2$	1100-1500	CO_2solubility	Infra-red absorption analysis of carbon
M.L.Pearce[34] (1964)	Na_2O-SiO_2	900-1300	CO_2solubility	Vacuum analysis
M.L.Pearce[35] (1965)	$Na_2O-B_2O_3$	900-1200	CO_2solubility	Vacuum analysis

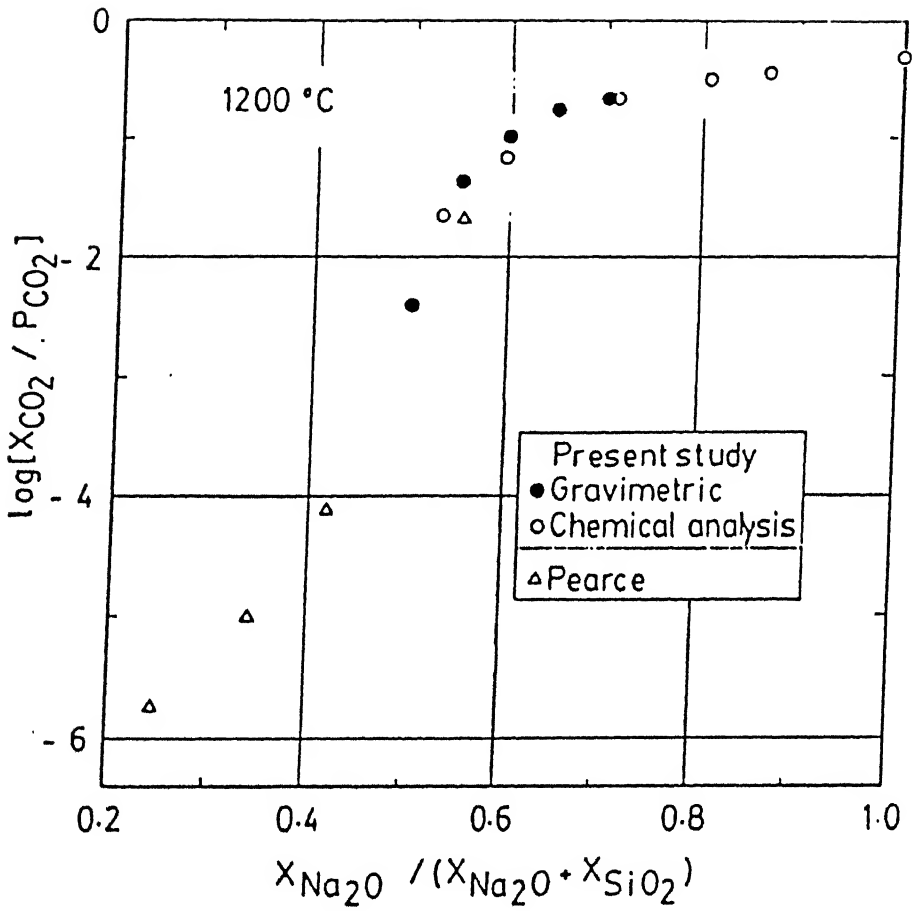

Fig. 2.6. A comparison of solubility data for carbon dioxide in sodium silicate melt at 1200°C[27]

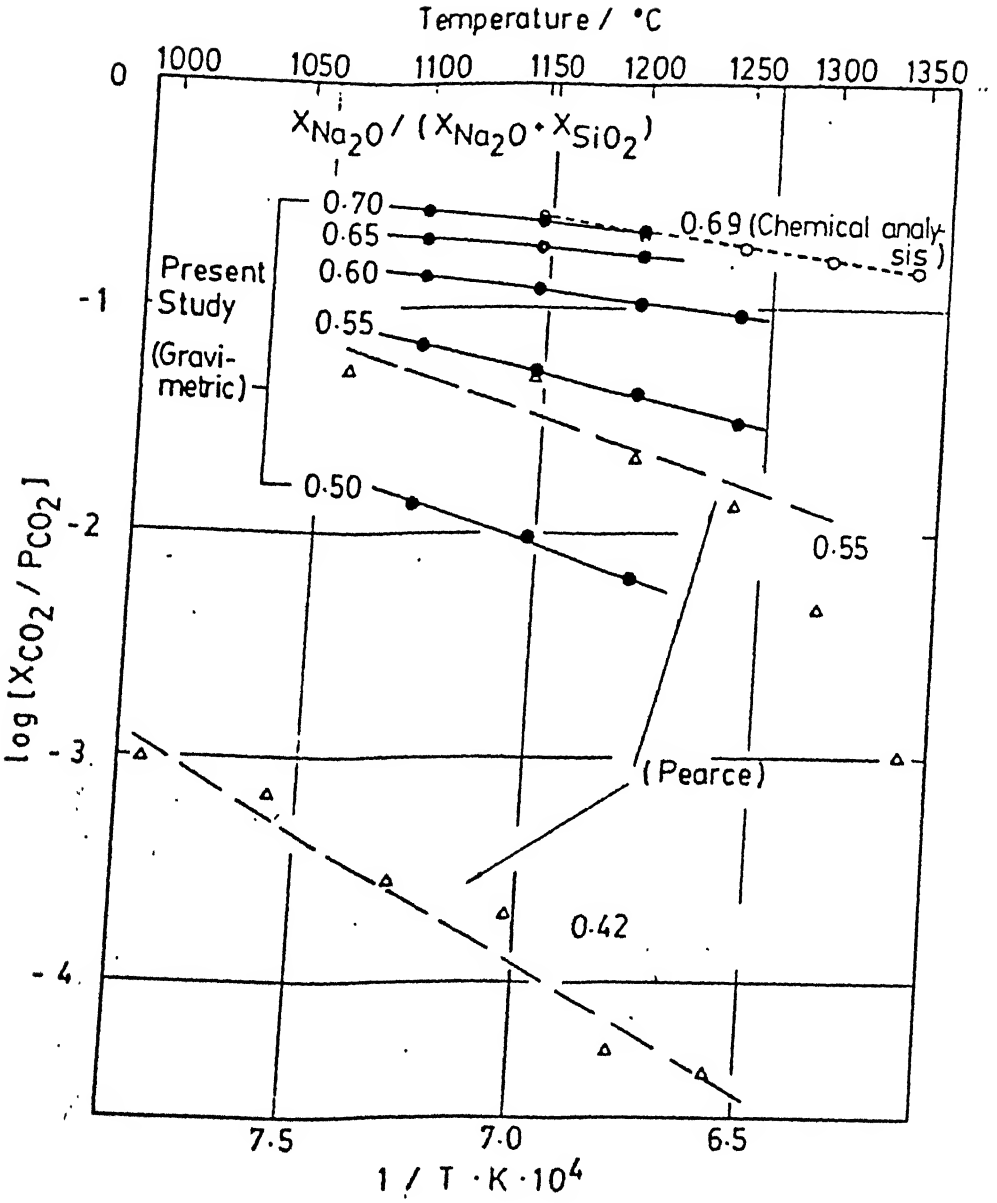

Fig. 2.7. Temperature dependence of CO_2 solubility in sodium silicate melts[27]

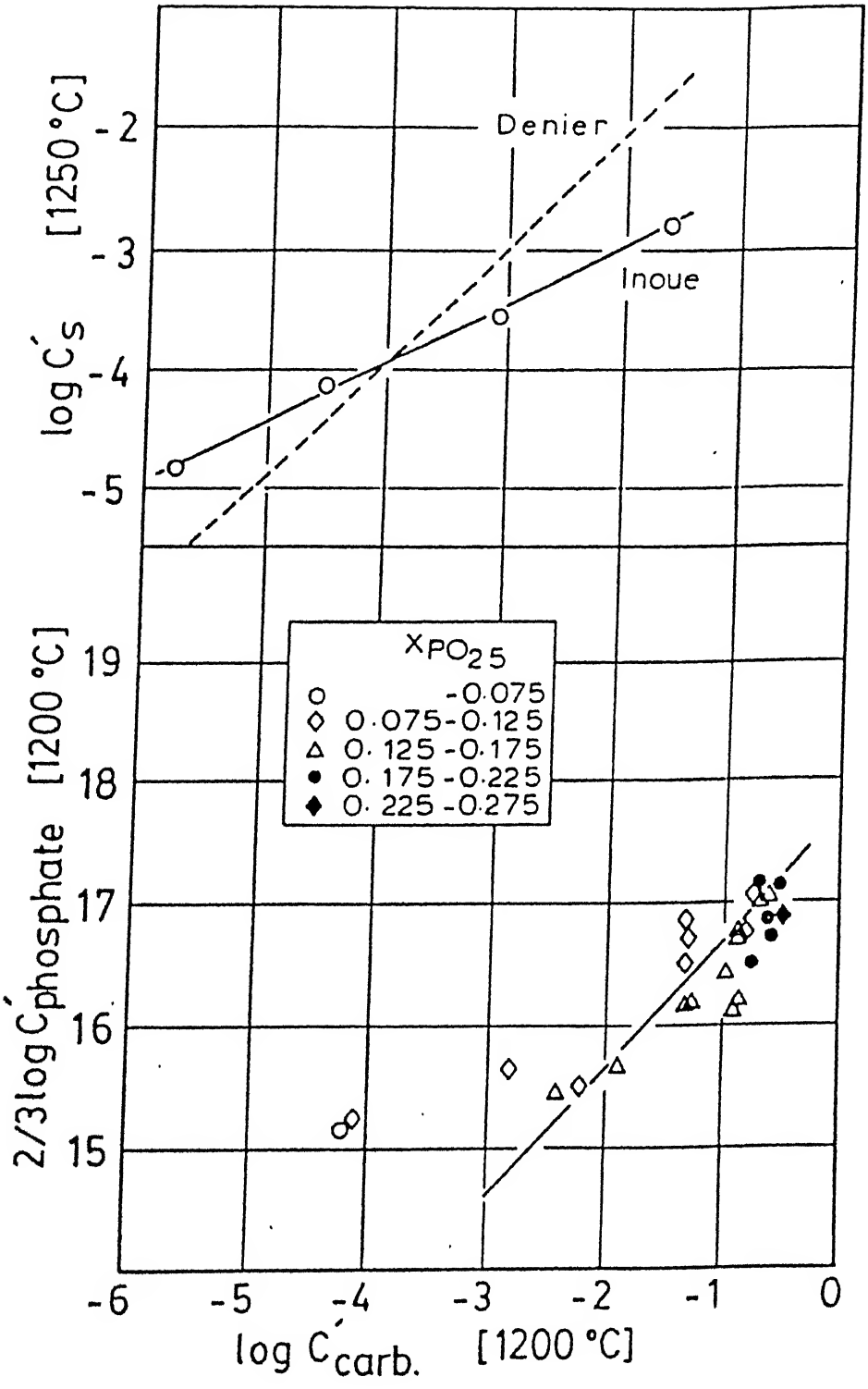

Fig. 2.8. Relationships among carbonate, sulphide, and phosphate capacities for sodium silicate melts[27]

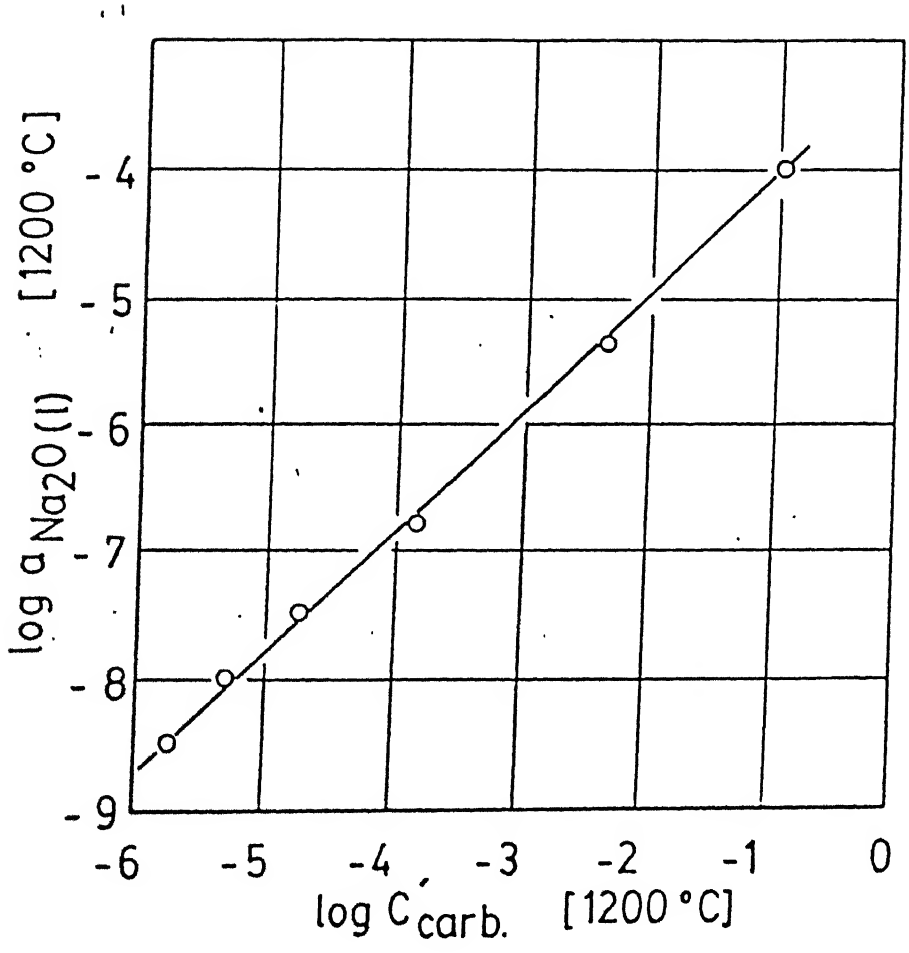

Fig. 2.0 The relationship between carbonate capacity and activity of Na_2O[27]

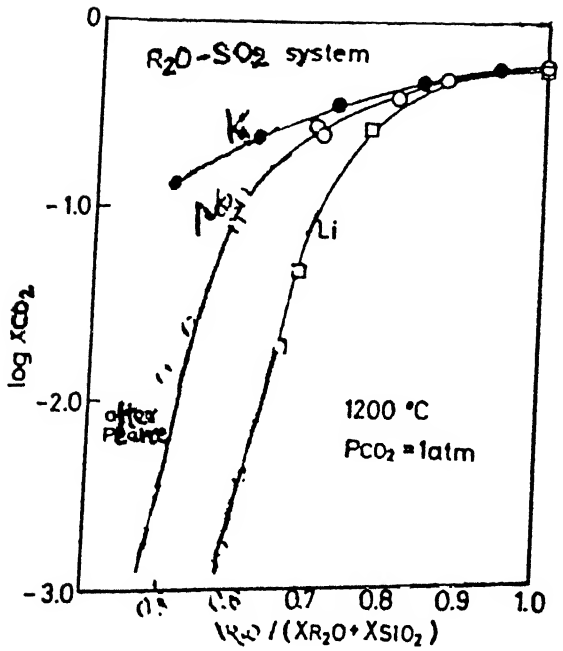

Fig. 2.10. CO_2 solubilities in melts containing alkali oxides at 1200°C[29]

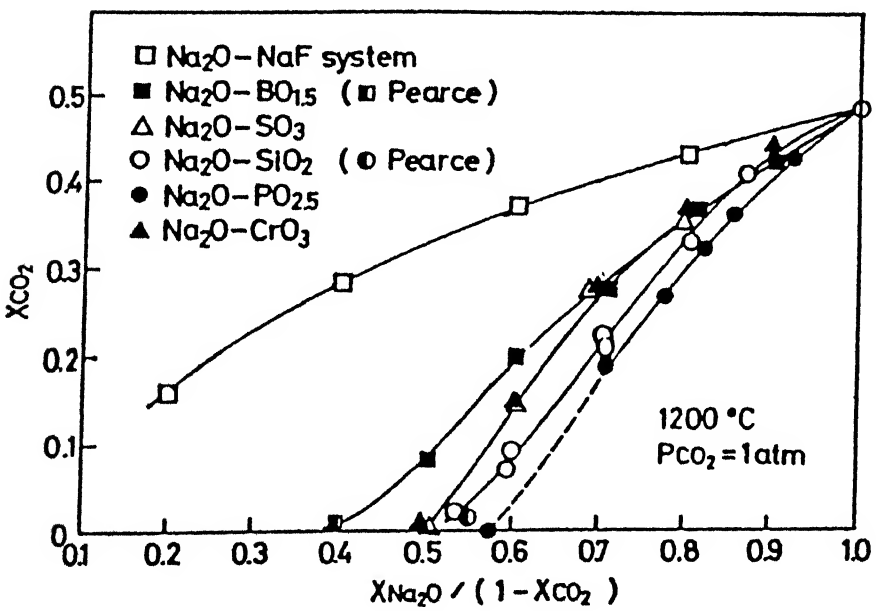

Fig. 2.11. CO_2 solubilities in the Na_2O- bearing melts at 1200°C[29]

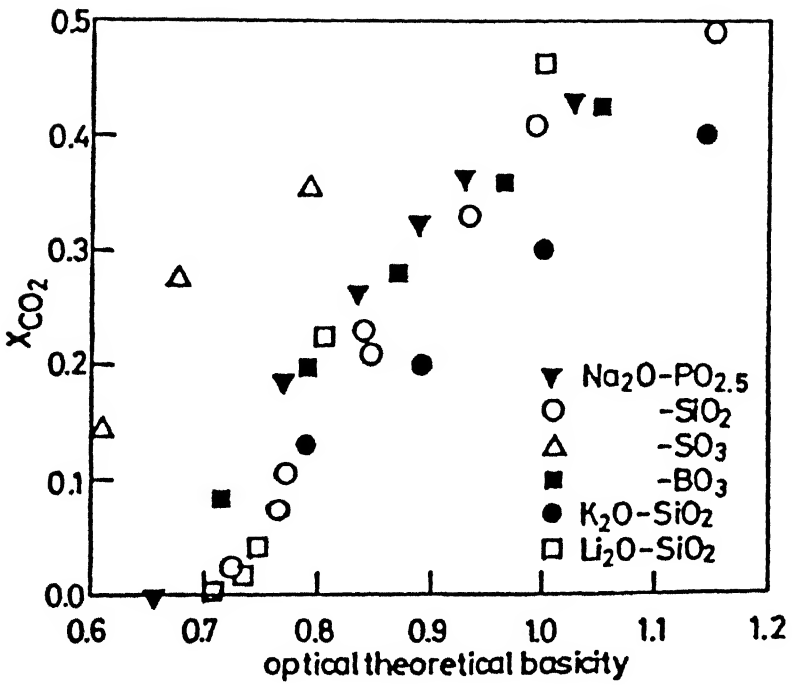

Fig. 2.12. CO_2 solubilities against theoretical optical basicity[29]

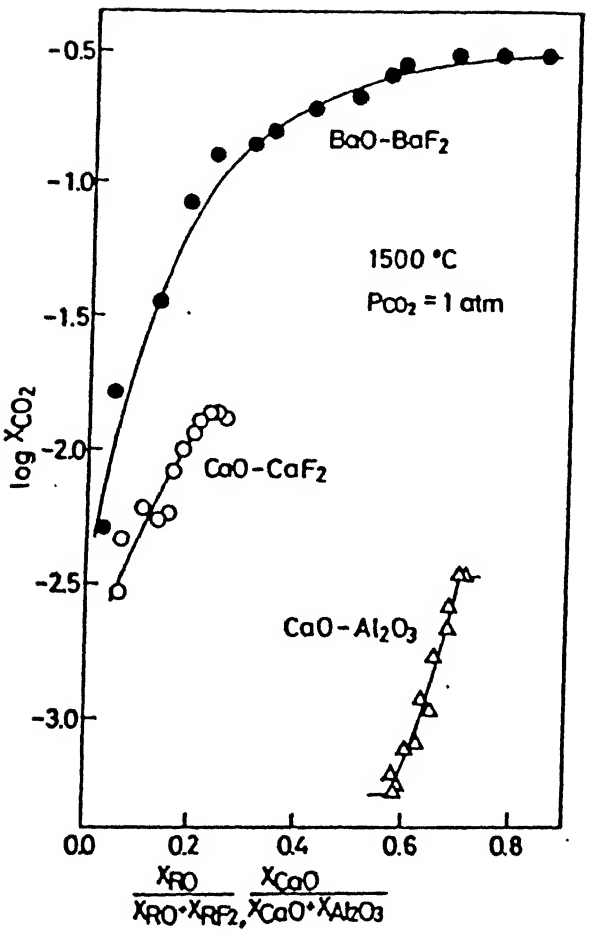

Fig. 2.13. CO_2 solubilities in the CaO-Al_2O_3, CaO-CaF_2 and BaO-BaF_2 melts at 1500°C[29]

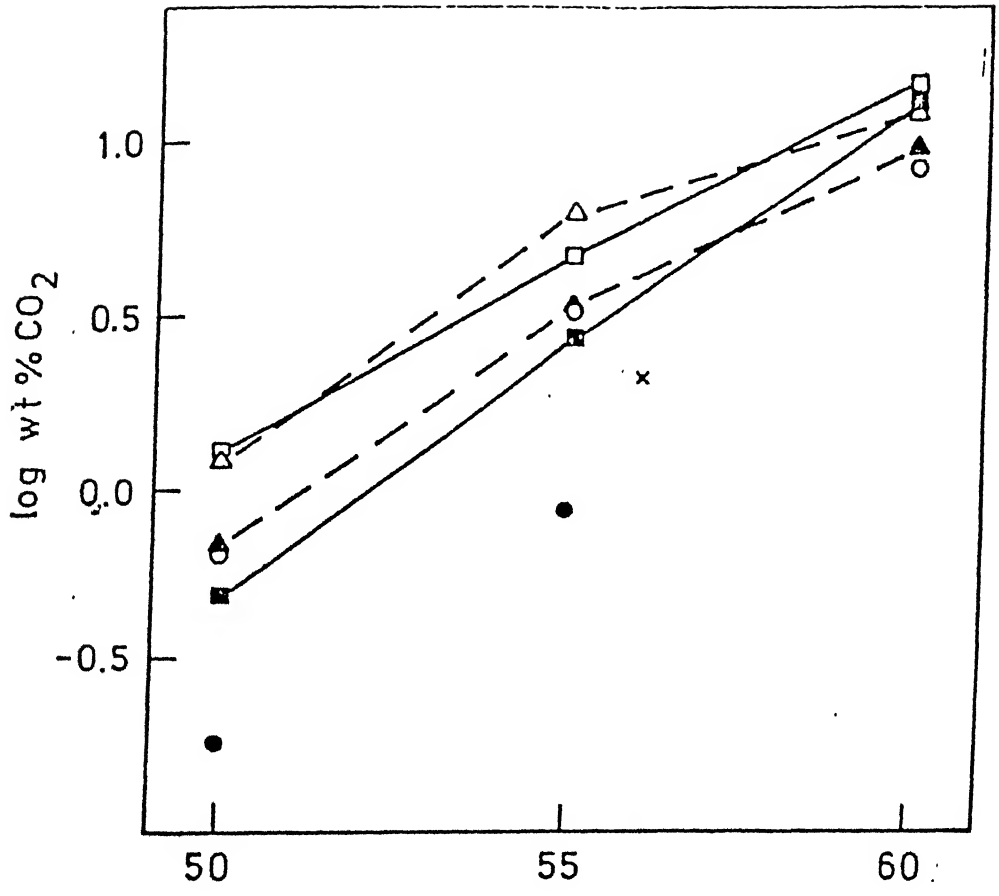

△1100 °C, ▲1200 °C } Maeda *et al.*[27]

○1100 °C, ●1200 °C } R. Berjoan and J. P. Coutures[39]

×1200 °C Pearce[34]

□1100 °C, ■1200 °C } Karvonen etal[30]

Fig. 2.14. CO_2 solubility in binary Na_2O-SiO_2 melts[30]

(Na^+, Li^+, Ba^{2+}, Sr^{2+} or Ca^{2+}) dissolved in liquid silicate.

Ikeda and Maeda[31] measured the C_c values by the thermogravimetric technique for $CaO-CaF_2-SiO_2$ molten fluxes at temperature from 1200°C to 1500°C. They found that C_c does not depend on the partial pressure of CO_2 gas as shown in Fig.(2.15). Fig.(2.16) shows that with increasing CaF_2 content upto 59.3 wt.pct., the C_c value increased but with further increase of CaF_2 C_c value decreased. But this increase or decrease of C_c value also depend upon the SiO_2 content of melt. They found a linear correlation between C_c and C_s as:

$$\log C_s = 1.1 \log C_c - 3.3 \qquad \ldots(2.47)$$

Maeda and Ikeda[32] used thermogravimetric technique to measure CO_2 solubility in molten $CaO-CaCl_2-CaF_2$ fluxes. Due to the vapourization of $CaCl_2$ weight loss occured. They have calculated the solubility of CO_2 after correcting the weight loss due to vapourization. Fig.(2.17) shows the replacement of $CaCl_2$ by CaF_2 at constant CaO mole pct, increased solubility of CO_2. They have also shown a linearity of C_c with C_s, C_N and C_p which are shown in Fig.(2.18), Fig.(2.19) and Fig.(2.20) respectively.

Pearce[34-35] has studied the CO_2 solubility in Na_2O-SiO_2 and $Na_2O-B_2O_3$ slags by vacuum analysis technique.

From all the above studies it is clear that there is linear correlation between C_c and other basicity sensitive parameters such as theoretical optical basicity, C_s, C_p, activity of basic oxides. Consequently we may say that the CO_2 solubility can be a good measure of slag basicity. Hence an extensive collection of C_c values for variety of fluxes is desired.

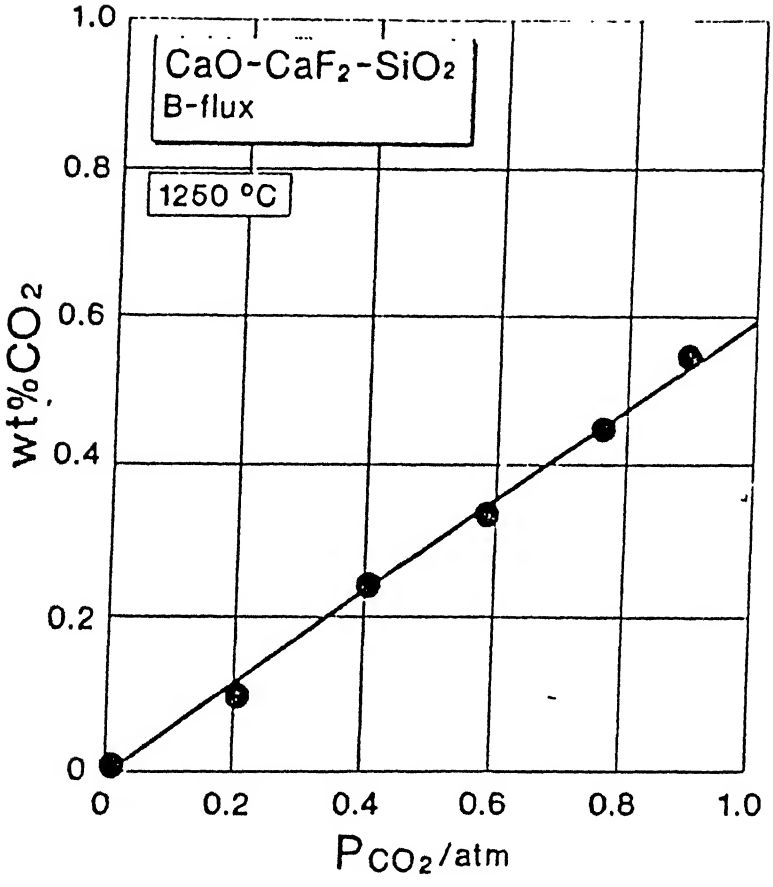

Fig. 2.15. Solubility of CO_2 in the slag of 39 wt pct. CaO-40 wt pct. CaF_2-21 wt pct. SiO_2 as a function of P_{CO_2} at 1250 ^{o}C[31]

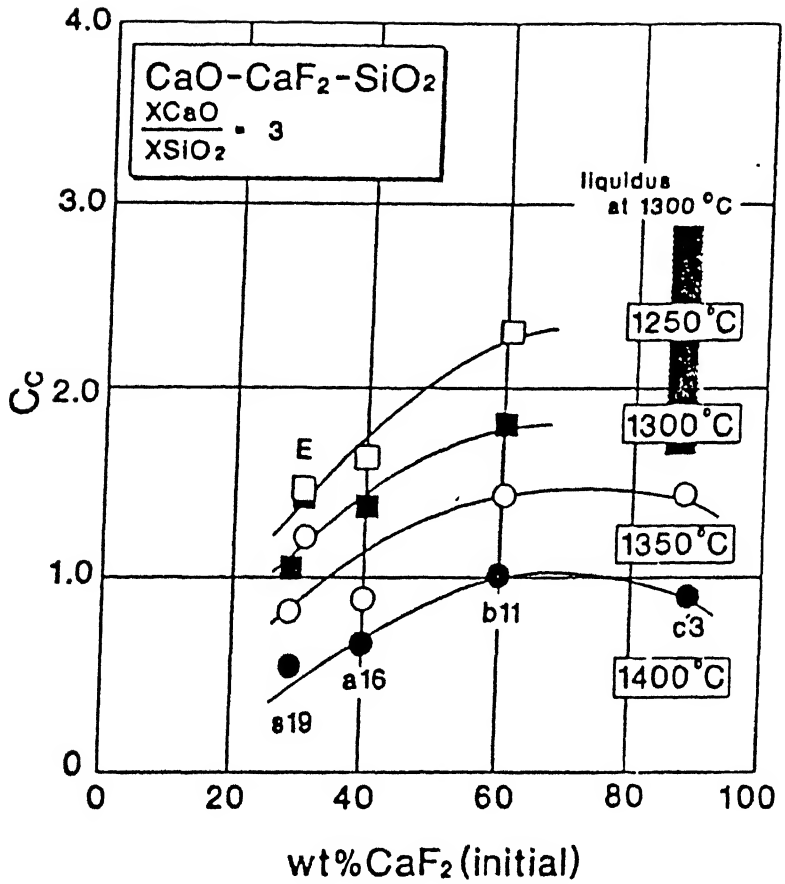

Fig. 2.16. Influence of CaF_2 on C_c at constant $X_{CaO} / X_{SiO_2} = 3$[31]

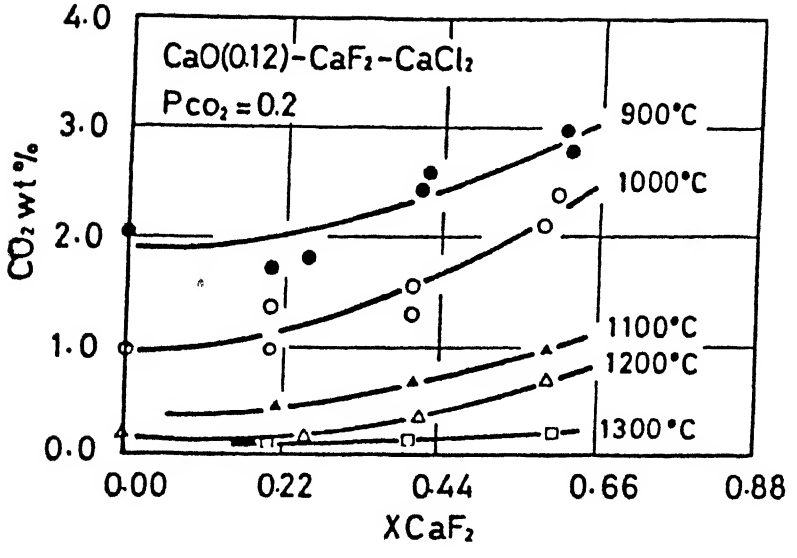

Fig. 2.17. Effect of CaF_2 addition in $CaO-CaCl_2-CaF_2$ melt at a fixed $X_{CaO} = 0.12$[32]

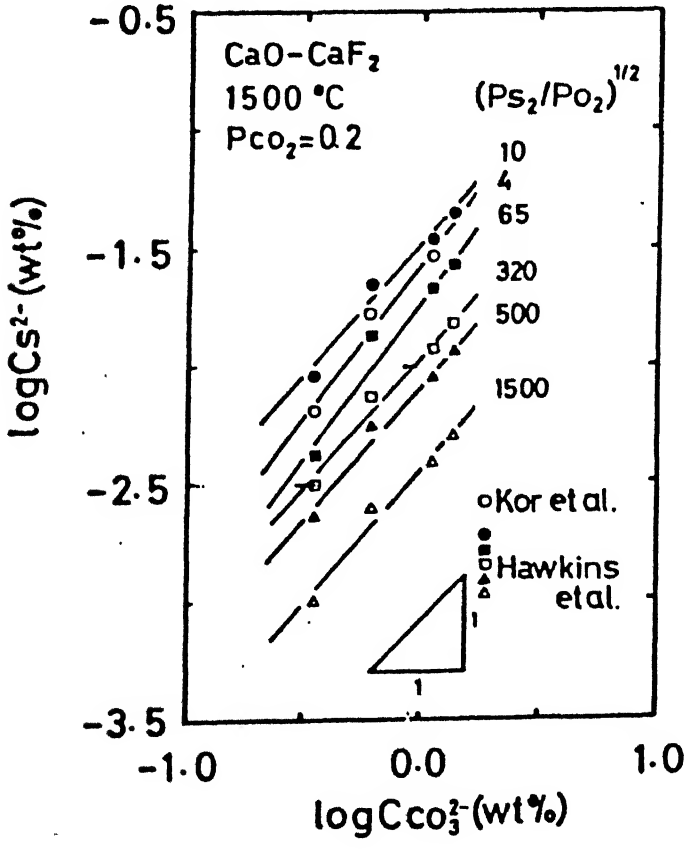

Fig. 2.18. Relationship between sulphide and carbonate

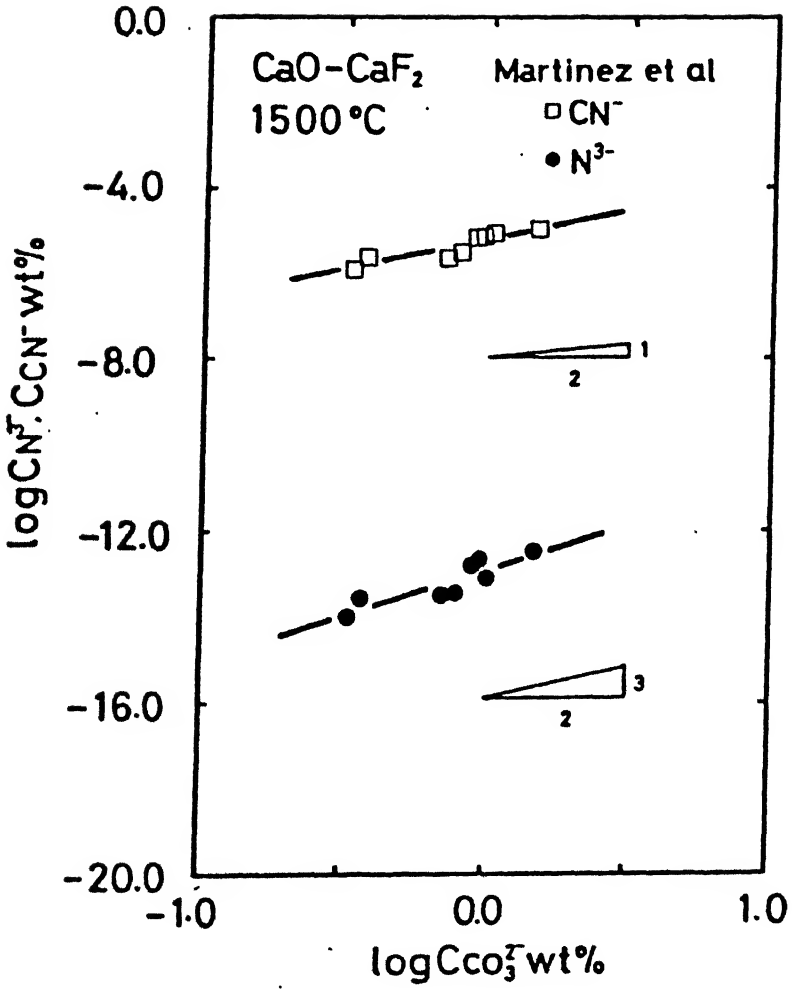

Fig. 2.19. Relationship between nitride and carbonate capacity of slag[32]

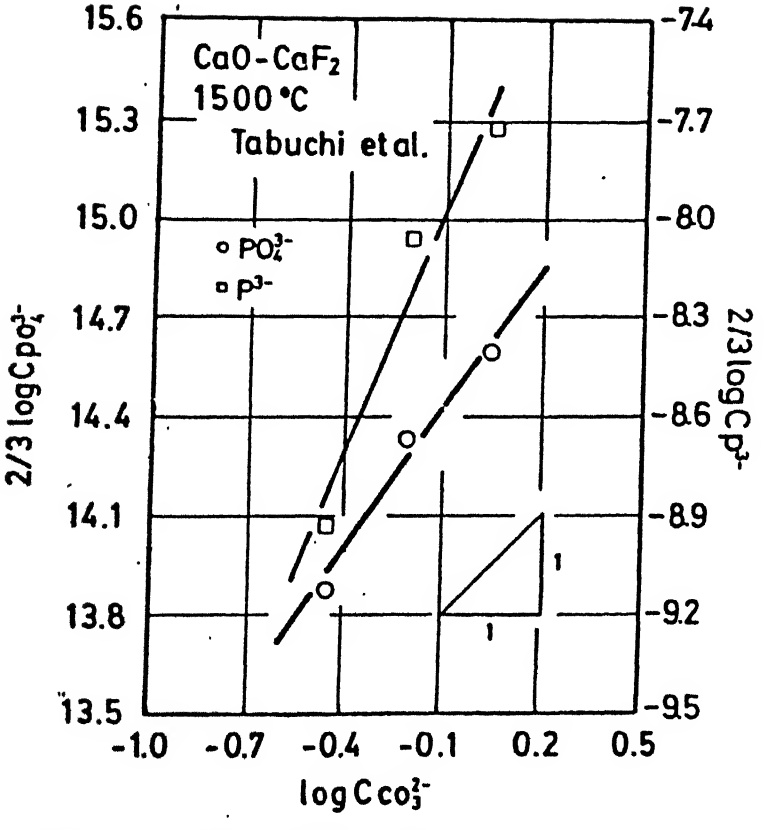

Fig. 2.20. Relationship between phosphate and carbonate capacity of slag[32]

CHAPTER 3

APPARATUS AND PROCEDURE

3.1 Apparats

3.1.1 Apparatus for slag making

It consisted of several apparatus but few which are more important are described below.

3.1.1.1 Slag melting furnace

The slag was melted in silicon carbide rod furnace. This furnace was designed and fabricated in the laboratory.

The heating elements of this furnace were six silicon carbide rods (Carborandum Corp., USA) having diameter of 2 cm and length 56 cm. These rods were fitted at equal distances on the periphery of a circle of 15.5 cm diameter. This was a vertical furnace of 55 cm height. A high temperature Mullite tube (5 cm inner diameter and 77 cm height), whose bottom side was closed, acted as reaction chamber. All the silicon carbide rods were connected in series. The temperature of the furnace was controlled by a continuously adjustable auto transformer (Dimmerstat, Automatic Electric Pvt. Ltd., Bombay). A chromel - Alumel thermocouple was inserted into the reaction chamber from the top opening, whose emf was measured by a 3-digit digital millivoltmeter (NAINA make).

3.1.1.2 Grinder

Grinder (FRUTSCH, puluriselte, Germany) was

employed for crushing and grinding of the solidified slags. It had a stainless steel ball of 5 cm diameter, and a semi spherical steel pot of diameter 9.3 cm. It was connected to 220V power supply. Magnetic field is produced by the AC current between the steel pot and steel ball. Due to this magnetic field, the steel ball rotates and vibrates in the semispherical steel pot and by this action sample is powdered.

3.1.2 Apparatus for measurement of carbonate capacity of slags

It consisted of a furnace, cahn electrobalance and gas train. These are described below.

3.1.2.1 Furnace

In this study a platinum-rhodium wound vertical tube furnace of 21 cm length was used. An alumina tube (17.5 mm inner diameter and 42 cm length) acted as reaction chamber. The alumina tube was fitted with two brass heads (one at the top and the other one at the bottom) to provide air tight fitting covers. The brass heads were attached with copper tube, and kept cooled by continuous flow of water through tubes. Thermocouple and gas inlet tube were inserted through bottom of the furnace. The temperature of the furnace was controlled to $\pm$ 1^{o}C by a power proportionating, indicating type temperature controller (Indotherm Instrument Pvt. Ltd., Bombay) actuated by a platinum - platinum -10% rhodium thermocouple. The thermocouple emf was measured by a 4-digit millivoltmeter (Vaiseshika Electron Devices, Ambala Cantt, type 7709). Silicone rubber `O' rings and high temperature silicone

sealant were employed to make the set up leak-proof.

3.1.2.2 Cahn electrobalance

Fig.3.1 shows the set up used for this study. The cahn 1000 (Cahn Instruments, USA) is an automatic recording sensitive electrical balance. It can weigh up to 100 gms and is sensitive to changes as small as 1 microgram as per specification. The balance is divided into two sections. One is the control-cum-output unit, and the other part is the weighing unit which detects the actual weight. The control unit was connected to a strip chart recorder (Digital Electronics Ltd., Bombay, Type : Omniscribe B 5000) to record changes of weight with time during the reaction.

3.1.2.3 Gas train

The basic purpose of the gas train was firstly to monitor the flow rate of the gases, and secondly to purify them from probable impurities present. Fig.3.2 presents the line diagram of the gas train.

Purified argon gas freed from moisture and carbon dioxide was employed for flushing and to maintain an inert atmosphere in the reaction chamber. Carbon dioxide gas freed from moisture was employed for absorption into the slag. Anhydrous calcium chloride ($CaCl_2$) and Drierite ($CaSO_4$) were employed for removal of moisture. Drierite has a lower equilibrium residual water vapour content as compared to anhydrous $CaCl_2$ and therefore it was used after the anhydrous calcium chloride column in the gas train for efficient removal of moisture. The Ascarite column after that of the Drierite in the argon line was meant for removal of

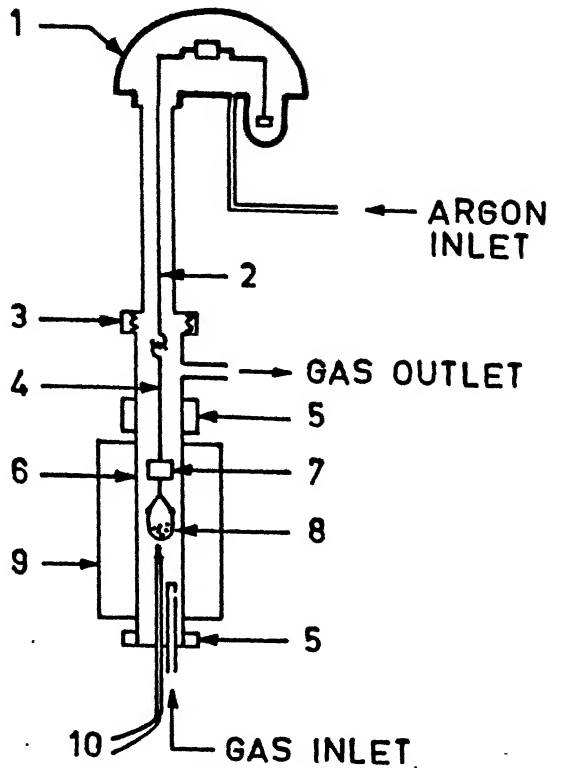

1 CAHN BALANCE
2 INCONEL ROD
3 SCREW CAP
4 HANGING ARRANGEMENT
5 COOLING ARRANGEMENT
6 ALUMINA TUBE
7 PLATINUM CYLINDER
8 PLATINUM CRUCIBLE WITH SAMPLE
9 PLATINUM-RHODIUM WOUND FURNACE
10 PLATINUM-PLATINUM-10% RHODIUM THERMOCOUPLE

Fig. 3.1. Schematic Diagram of the Thermogravimetry Setup with Cahn Electrobalance.

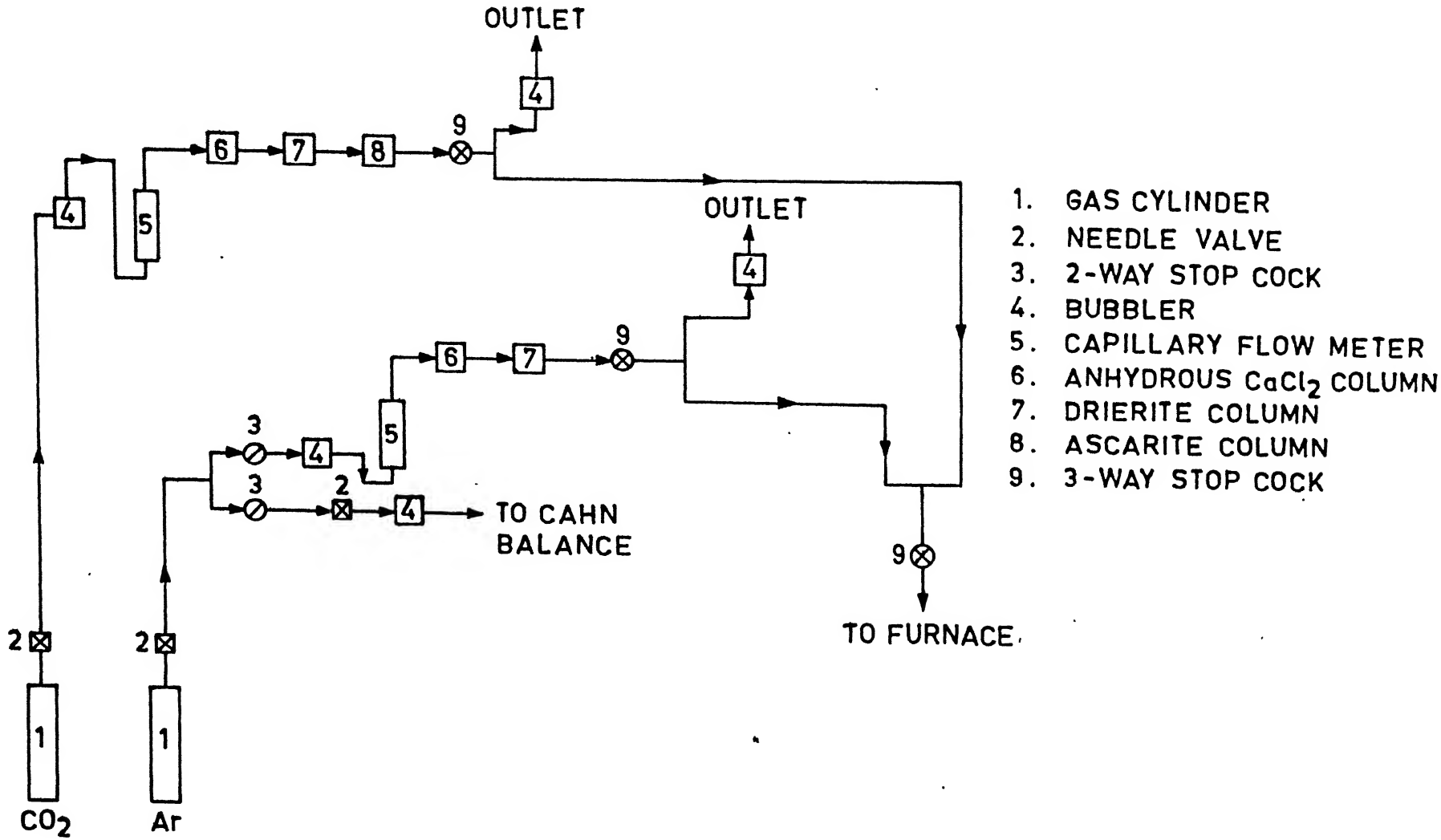

Fig. 3.2. Schematic Diagram of the Gas Train Used with Thermogravimetry Setup.

the carbon dioxide present.

The capillary flow meters had been designed and fabricated in this laboratory earlier for measuring very low flow rates (maximum 1 $cm^3 S^{-1}$). Calibrations of the individual flow meters were done. Results are being presented in Table 3.1 in equation form after data fitting by linear regression. Here Q is the flow rate of gas in $cm^3 S^{-1}$ (STP) and h is the height difference in centimeter.

Table 3.1 : Calibration equation for flow meters

Gas	Flow meter (No.)	Equation
CO_2	1	Q = 0.2960h + 0.249
Ar	2	Q = 1.0319h + 0.479

Experimental Procedure

3.2.1 Procedure for slag making

The chemicals used in this study are listed in 3.2.

Table 3.2 : Chemicals used in the present study

Chemicals	Chemical Formula	Purity pct.	Company
Ortho boric acid	H_3BO_3	99.94	FISHER SCIENTIFIC COMPANY (USA)
Calcium carbonate	$CaCO_3$	99.5	THE BRITISH DRUG HOUSES LTD. (England)
Silica	SiO_2	99.9	FLUKA (Switzerland)
Sodium carbonate	Na_2CO_3	99.9	THOMAS BAKER PVT. LTD. (Bombaay)
Calcium flouride	CaF_2		E. MARK, DARMSTADT (Germany)

The slag making operation consisted of following steps:

(i) removal of moisture from chemicals,

(ii) decomposition of orthoboric acid to boron trioxide,

(iii) calcination of lime stone,

(iv) melting of slags,

(v) cleaning of platinum crucible,

(vi) crushing and grinding of slags and

(vii) proper storage and subsequent handling.

3.2.1.1 Removal of moisture from chemicals

The chemicals used contained moisture and volatile matters, which should be removed before melting.

Each 150 grams of chemicals were taken in different glass pertri-dishes. After keeping twelve hours at 120°C in an oven, the dishes containing chemicals were taken out. The chemicals were kept in plastic bottles after cooling and then these bottles were kept in desiccator.

3.2.1.2 Decomposition of orthoboric acid t boron trioxide

The decomposition of orthoboric acid takes place in different steps at different temperatures[36].

At 100°C, the acid loses water and is converted into metaboric acid

$$H_3BO_3 = HBO_2 + H_2O \qquad ...(3.1)$$

At 140°C, metaboric acid gets converted into pyroboric acid

$$4HBO_2 = H_2B_4O_7 + H_2O \qquad ...(3.2)$$

At higher temperature all the water is lost and

boron trioxide is formed

$$H_2B_4O_7 = 2B_2O_3 + H_2O \quad \ldots(3.3)$$

Several trials were given at various temperatures in a muffle furnace. Finally at 500°C, it was found that the evolution of water vapour takes place at fast rate, and B_2O_3 was obtained in liquid form.

At higher temperature, B_2O_3 comes out from the container by creeping due to its wetting characteristics. It was found that if the decomposition of ortho boric acid was done in glass beaker and if this beaker was removed from the furnace at decomposition temperature, the glass beaker cracked. Hence the B_2O_3 containing container should be cooled down in the furnace.

3.2.1.3 Calcination of limee stone

At 1 atmospheric pressure, the decomposition of $CaCO_3$ takes place at approximately 900°C[36]. This is an endothermic process. The calcination of lime stone takes place by the following reaction.

$$CaCO_3(s) = CaO(s) + CO_2(g) \quad \ldots(3.4)$$

The rate of calcination seems to be primarily governed by the supply of necessary heat of decomposition.

A weighed amount of dried $CaCO_3$ powder was taken in an alumina crucible, and it was placed in a silicon carbide pit furnace initially at lower temperature. Then temperature was slowly increased to 1000°C with the help of controller. After keeping for 12-14 hours at that temperature, the crucible was taken out and weights were taken after cooling. It was found that the calcination was not complete. The rate of calcination depends

also upon the bed thickness. Hence a small amount of dried $CaCO_3$ powder was taken and kept at higher temperature (i.e. 1100°C) for 12 to 14 hours. It was found that the calcination was complete. Then this calcined CaO, which was in spongy and lumpy form was broken and kept in desiccator.

3.2.1.4 Melting of slags

Initially the base composition of slags chosen were (by weight ratio):

$CaO-B_2O_3-SiO_2$ (5:3:2) and $CaO-B_2O_3-SiO_2$ (5:4:1). Subsequently more compositions were prepared by adding 5 pct., 10 pct. and 20 pct. CaF_2 by weight.

First the weighed amount of CaO was taken in a platinum crucible and introduced into the silicon carbide furnace, which was maintained at 1100°C. After one hour it was taken out and weight taken after cooling. This process causes the removal of any residual CO_2 remaining as $CaCO_3$ in the already calcined sample.

Then the different constituents of slag were taken in the platinum crucible in weighed quantities and these were properly mixed by a glass rod. This platinum crucible was introduced in the silicon carbide furnace and was kept there at 1200°C for 2 hours. The molten slag was stirred by an Inconel wire for proper mixing, and then again left for one hour in the liquid state. Then the crucible was taken out from the furnace by an Inconel wire and the slag was poured onto a cleaned copper sheet.

$Na_2O - SiO_2 - B_2O_3 - CaO$ of varying composition were melted by adding the proper weights of sodium carbonate, silica, boron trioxide and calcium oxide. Sodium carbonate has very high

decomposition temperature at one atmospheric pressure. Hence it was not possible to decompose it to Na_2O prior to use.

3.2.1.5 Cleaning of platinum crucibles

The slags were melted in platinum crucible. This crucible should be properly cleaned for melting of next slag composition. The cleaning of crucible was done by hydrochloric (HCl) and hydrofluoric (HF) acid mixture. First dilute HCl was taken in the crucible and then HF was added. Then the crucible was kept on a hot plate inside a fume hood.

The slag system $CaO - SiO_2 - B_2O_3$ caused lot of problem in cleaning. The acid attack on these slags was only in thin layer, which was washed in water, and again acids were added. This way crucible was cleaned. Therefore the crucible was first inverted into the furnace for the residual slag to flow out and the rest cleaned by acid. It took shorter time. Cleaning of $Na_2O - SiO_2 - B_2O_3 - CaO$ slags was not so difficult. These slags were soluble in water also. Cleaning by water takes much time, but the crucible was cleaned easily by acid.

3.2.1.6 Crushing and grinding of slags

The solidified slags were in lumpy form which should be crushed and ground. This was done in the Grinder. The steel ball and semi-spherical steel container were properly cleaned with water and finally with acetone. Then the slag was kept in the pot and the chamber was closed. The Grinder was kept on for 30-40 minutes, then the ground slag was taken out and kept in oven at $120^{\circ}C$ for 12-14 hours. Then it was taken out, and after cooling stored in desiccator.

3.2.2 Procedure for measurement of carbonate capacities of slags

The existing Cahn balance set up has been described in section 3.1.2. Several trials were carried out before arriving at the actual experimental procedure. Argon gas was directly passed into the furnace through anhydrous calcium chloride, Drierite and Ascarite columns. Carbon dioxide was passed through anhydrous Calcium chloride and Drierite columns only for removal of moisture.

The hanging assembly is shown in Fig.3.3. A platinum crucible (10 mm diameter and 10 mm height), in which slag can be kept was hanged by a thin platinum wire. A platinum cylinder (12 mm diameter and 10 mm height) was attached to platinum wire and positioned above the crucible. The cylinder kept the hanging assembly vertical and straight.

Experimental procedure is noted below.

(i) The Cahn balance was switched on at least eight hours before performing the actual experiment. This was done for stabilizing the control unit of the balance.

(ii) The furnace temperature was stabilized at the set value by the temperature controller.

(iii) Recorder was also switched on at least 30 minutes before recording.

(iv) Argon gas flow was started through the furnace chamber as well as the weighing unit of the balance at fixed flow rates.

(v) The crucible containing weighed amount of slag was

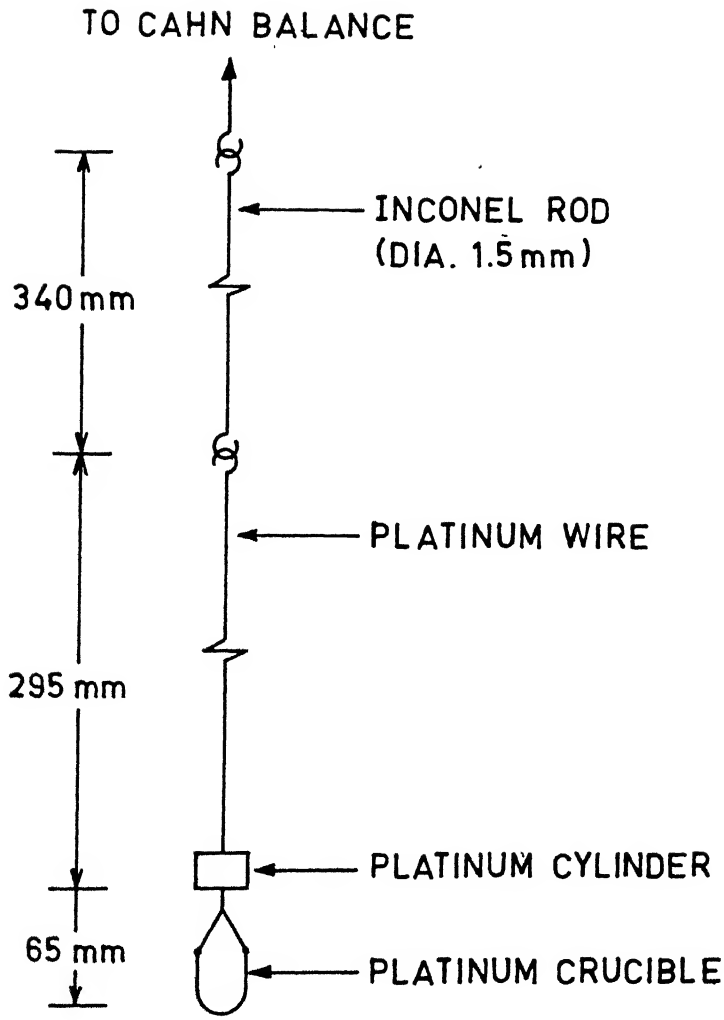

Fig. 3.3. Hanging Assembly for Thermogravimetry.

introduced into the hot zone of the furnace.

(vi) The furnace was lifted and screwed with top hanging glass tube, which keeps the reaction chamber leak proof.

(vii) The weight suppression range (WSR) and meter and recorder range (MRR) were set at 10 gms and 10 mg respectively, and weight suppression was carried out.

(viii) The output was continuously recorded on recorder chart.

(ix) The gas through the furnace was changed to carbon dioxide at fixed flow rate after 60 to 90 minutes.

(x) The argon flow through the balance was maintained at the same rate. This procedure was to ensure better environment for the balance chamber. Since the gas exit was located far above the furnace (Fig.3.1) and the argon flow rate through the balance was low (approximately 30 to 40 cm^3/min^{-1}), it cannot affect the purity of CO_2 flowing through the furnace in any significant way.

(xi) At the same temperature, the sample was kept in CO_2 atmosphere at least for 100 to 150 minutes for equilibrium to establish between CO_2 and oxygen ion (O^{2-}), and the differential weight data were recorded automatically as function of time.

(xii) Then the CO_2 gas was changed to argon again at the same flow rate and the temperature was increased by 50^oC.

(xiii) As above, at different temperatures at 50^oC interval, the experiment was carried out and differential weight data were recorded.

After some weight gain, the sample started to lose weight in the carbon dioxide atmosphere. It was thought that this might be happening due to presence of impurities in carbon dioxide. Commercial carbon dioxide is produced as a by-product of fermentation of molasses, and contains many organic volatile impurities such as alcohols, ketones, aldehydes etc. Methods to purify such impure carbon dioxide have already been in practice commercially on a large scale. One of the methods, known as the Backus process[37], has been found simple and suitable for the laboratory. The purification system consists of a number of scrubbers in a sequence through which impure carbon dioxide is made to pass. Backus process had been previously used in author's laboratory by others, and the basic set up was available. It was cleaned and fresh chemicals were used.

After connecting the Backus train in CO_2 gas line, no difference was found in the recorded data for same slag composition, temperature, and gas flow rate. Hence the Backus unit was removed from the CO_2 gas line. Ultimately it was concluded that the weight loss was due to volatilization of some components of slag. The chapter on Result and Discussions would provide details as to how corrections were incorporated for this.

Problems encountered during experiments were as follows.

(i) Disruption in power and water supply led to abandonment of several experiments.

(ii) Touching of the platinum crucible and cylinder with inner tube of the furnace causes too much fluctuation.

The whole hanging assembly should be free from touching. This was achieved for several experiments by successive trials, but there were many failures as well.

(iii) The slag deposited into the inner tube of the furnace after volatilization affected the freedom of hanging crucible and cylinder. Attempts were made for cleaning these time to time, but the deposits were so hard that complete cleaning was not possible.

(iv) Due to wetting of platinum crucible by the melt, the latter creeps out of the crucible.

(v) The control unit of cahn balance, during summer caused lot of problems due to high room temperature. Specially the Weight Suppression (WS) behaved erratically.

CHAPTER 4

RESULTS AND DISCUSSIONS

4.1 Slag Compositions

Table 4.1 presents compositions of all the slags prepared by melting for the present investigation. Chapter 3 has already described the procedure for making slags.

Criteria for selection of slag systems were as follows.

(i) Melting point should be less than 1100^{o}C in order to accommodate the furnaces available in the laboratory.

(ii) The systems should be such that there is no major repetition with literature data.

(iii) Solubility of CO_2 should be less than 1 wt.pct. so that Henrian behaviour can be assumed.

(iv) The slag should be fluid at experimental temperature so that it does not take a very long time to saturate with the carbon dioxide.

(v) In this study vapourization of oxides and consequent loss of weight is a source of error and therefore compounds selected for slag making should have low vapour pressure if possible.

Keeping in mind the above criteria, specially (i) and (ii), it was decided to carry out measurement of carbonate

Table 4.1 : Compositions of slag prepared

Sr. No.	mole pct.				
	Na_2O	SiO_2	B_2O_3	CaO	CaF_2
1.	60	40	-	-	-
2.	60	-	40	-	-
3.	50	50	-	-	-
4.	50	40	10	-	-
5.	50	30	20	-	-
6.	50	20	30	-	-
7.	50	10	40	-	-
8.	50	-	50	-	-
9.	50	40	-	10	-
10.	50	-	40	10	-
11.	50	20	20	10	-
12.	-	10.2	35.2	54.6	-
13.	-	20.1	26.0	53.9	-
14.	-	9.8	33.7	52.2	4.3
15.	-	9.3	32.3	49.7	8.7
16.	-	8.2	28.9	44.7	18.2
17.	-	19.4	24.9	51.5	4.2
18.	-	18.4	23.9	49.1	8.6
19.	-	16.8	21.1	44.1	18.0

capacity of slags based on boron oxide (B_2O_3), which have low liquidus temperature. Search of literature also showed relevance of these melts as slags, fluxes and glass. Moreover not much measurement of carbonate capacity have been done on them.

Two slag systems were selected.

(i) $CaO-B_2O_3-SiO_2$ with or without addition of CaF_2; in this system phase diagram was consulted[38] for low melting region and based on the same the following two master slags were chosen.

the entire duration of the measurement program, the power and water supply were getting interrupted and that too without any prior notice. This led to delay as well as failures of many experiments.

(ii) In the summer month, the balance often exhibited erratic behaviour causing failure of a number of measurements.

(iii) Oscillation of the crucible assembly containing slag was a problem. This was due to a long hanging wire and gas flow through the reaction chamber. Such oscillation caused oscillation in recorder pen as well as touching of the crucible assembly to the furnace wall. It was minimized by fixing a platinum cylinder above the crucible. Even then touching remained a problem especially towards the end of the experimental program due to the deposition of slag vaporized from the sample.

(iv) Vapourization of components of slag made measurements difficult. It also increased the touching problem due to slag deposition on the wall of the alumina tube and the brass heads. Cleaning was very difficult and attempt to do so led to damage to the furnace finally. Vapourization also did not allow experiments at higher temperatures.

Temperature was controlled by a power proportionating,

indicating type temperature controller (Indotherm Instruments Pvt. Ltd., Bombay) within $\pm$ 1^{o}C. The temperature was also continuously measured by a 4-digit precision milivoltmeter within $\pm$ 2^{o}C. The digital milivoltmeter was calibrated against a primary calibration source.

For weight change measurements, the change of weight was continuously recorded in the recorder chart. Range of recorder was set at 10 mg weight, giving a sensitivity of measurement of weight change of 0.05 mg. This sensitivity was quite good. The recorder calibration had been initially checked by a calibrated 100 mg weight, and later from time to time with the digital weight suppression facility of control unit. Gas flow rates were known from calibrated capillary flow meters. Total pressure was 1 atm inside the reaction tube, and was approximately equal to 1 bar.

The various sources of uncertainty in measurement of weight gain of slag due to absorption of carbon dioxide were considered. The buoyancy effect due to change of gas from argon to CO_2 was estimated as negligible. The sources affecting weight change significantly were found to be:

(i) upward drag force on crucible due to flow of gas through the furnace tube,

and (ii) volatilization of components of slag.

These could not be eliminated experimentally. Hence corrections were made to determine extent of dissolution of CO_2 in slag. These are being discussed below.

4.2.2 Drag force and its correction

Fig.4.1 illustrates occurrence of upward drag due to gas flow and its effect on sample weight. The drag force causes loss of weight of crucible assembly; as Fig.4.1 shows that when CO_2 was started there is a sudden shift of the pen in the recorder due to weight decrease as a consequence of drag. Then the recorder shows rapid weight gain. The initial decrease however was not entirely due to drag force, but to quite an extent due to inertia of the recorder pen and measuring unit. Therefore in order to find out the correct weight gain the drag force due to flow of CO_2 is to be added to the weight gain as a result of carbon dioxide absorption.

Hence the following procedure was followed as illustrated in Fig.4.1.

(i) The weight was balanced by digital weight suppression facility in balance, and stable recorder reading was obtained under argon at known flow rate for approximately 60 to 90 minutes.

(ii) Argon flow was suddenly stopped and the weight was recorded in static argon for sometime.

(iii) The flow of CO_2 at fixed flow rate had already been stabilized through a bypass. Now the stop cock was operated so as to pass the gas through the furnace chamber. The experiment was carried out under flowing CO_2 as long as necessary.

(iv) Then CO_2 was suddenly stopped and weight was recorded in static CO_2. From this the drag force

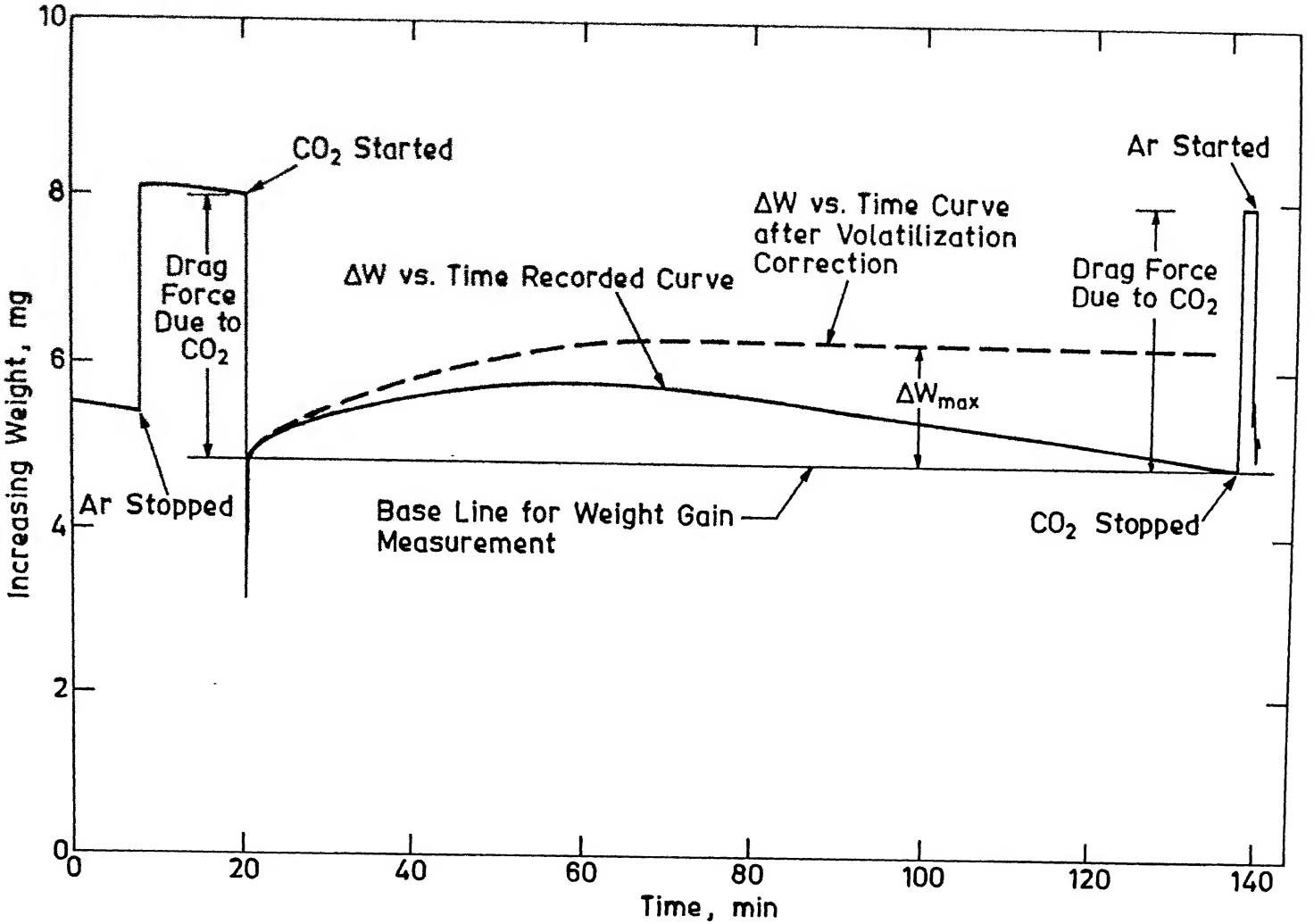

Fig. 4.1. Weight Gain versus Time Plot for $50Na_2O-50SiO_2$ Melt.

of flowing CO_2 was measured as shown in Fig.4.1. This drag force was subtracted from the initial weight in static argon to obtain a base line for weight gain measurement.

Some experimental data on drag force measurements both in argon as well as CO_2 to have been compiled in Table 4.2. It was decided to calculate the drag force theoretically expected by assuming the simplest possible situation i.e. flow of gas assuming the crucible to be an equivalent sphere. Appendix shows a sample calculation. Table 4.2 presents calculated values of drag force.

Table 4.2 : Values of drag force in some experiments

Expt. No.	Temp. °C	Argon			Carbon dioxide		
		Gas flow rate, $cm^3 S^{-1}$ (STP)	Drag force, mg weight		Gas flow rate, $cm^3 S^{-1}$ (STP)	Drag force, mg weight	
			Estimated	Experimental		Estimated	Experimental
1.	1100	1.42	0.016	2.16	2.92	0.035	2.84
2.	1250	1.42	0.018	2.20	3.33	0.048	3.12
3a.	1100	1.67	0.019	2.48	3.33	0.042	3.04
3b.	1150	1.67	0.020	2.64	3.00	0.041	2.72
3c.	1200	1.67	0.021	2.68	3.33	0.046	3.12
3d.	1250	1.67	0.022	2.96	3.33	0.048	3.36
4a.	1100	3.33	0.052	5.60	3.33	0.042	3.12
4b.	1150	3.33	0.054	6.00	3.33	0.044	3.36
4c.	1200	3.33	0.057	6.40	3.33	0.046	3.60
4d.	1250	3.33	0.059	6.56	3.33	0.048	3.68
5a.	1000	3.33	0.047	5.68	3.33	0.038	3.36
5b.	1050	3.33	0.049	6.56	3.33	0.040	3.84

Table 4.2 reveals that calculated values of drag force are two orders of magnitude less than the experimentally obtained

values. Fig.4.2 shows the relationship graphically for many experiments. The following points may be noted in this connection.

(i) There is lot of scatter in experimentally measured values at higher flow rates.

(ii) For CO_2, experimental values did not show any correlation with estimated values.

(iii) For argon, straight line relationship was obtained at low flow rates and the points at high flow rates scattered around this line.

It may be assumed that the discrepancy between experimental and calculated values is largely due to the fact that the calculations were performed for a sphere over which the gas was flowing in an open space. However the geometry of the crucible assembly was not spherical. Also there was wall effect due to presence of the reaction tube surrounding the crucible, and the associated complications. The above remarks are tentative only.

4.2.3 Correction for volatilization loss

Fig.4.1 shows a sample recorder trace for absorption experiment (expt no. 4b) for 50 mole pct. Na_2O-50 mole pct. SiO_2 slag at 1150°C temperature. It may be noticed that during flow of CO_2 the weight reached a maximum, and then started to decrease. This is because the CO_2 absorption responsible for weight gain was quite fast. However weight loss due to volatilization continued continuously, and was responsible for this nature of curve. It may also be noted that weight loss was constant as may be concluded

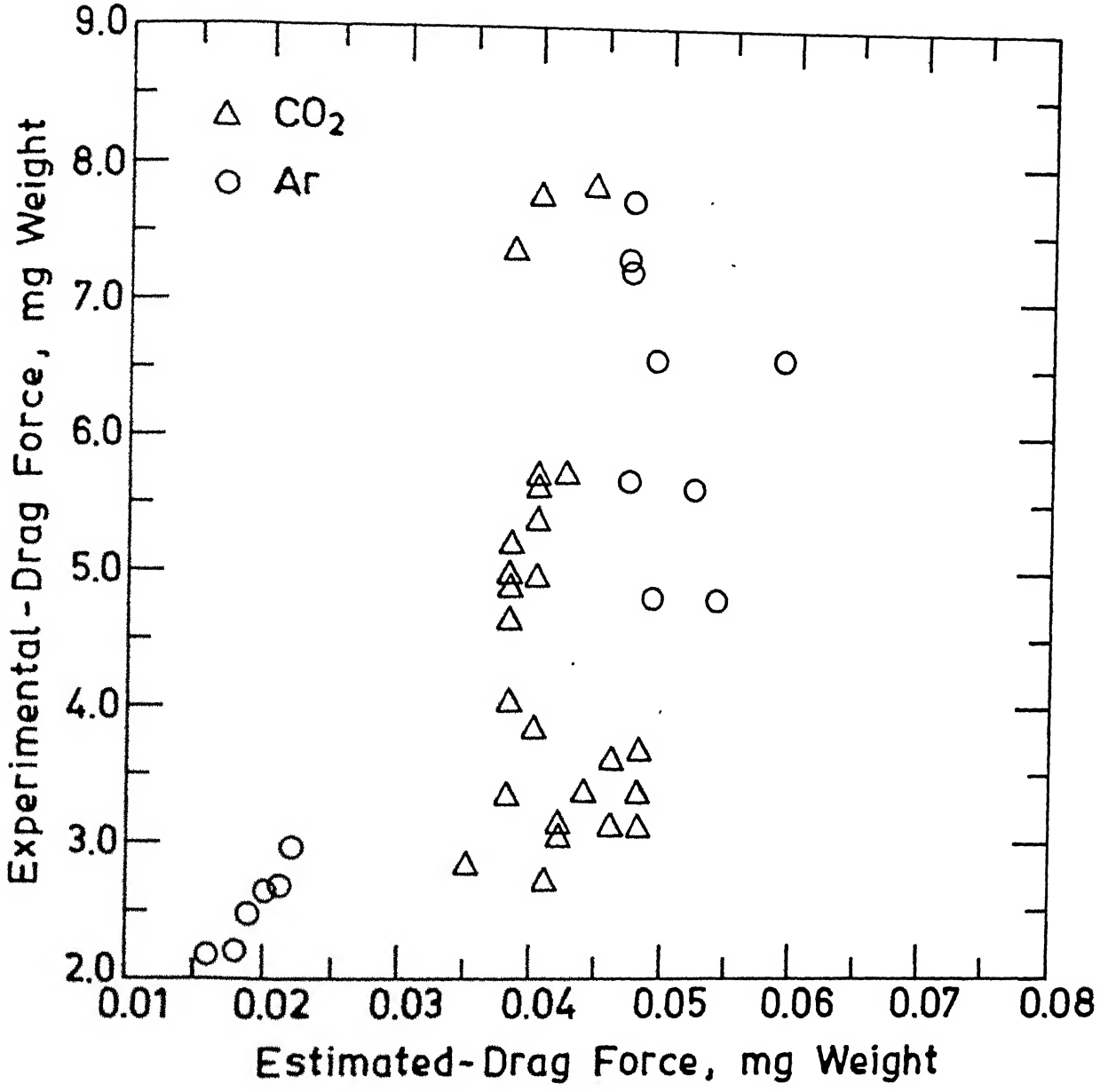

Fig. 4.2. Estimated Drag Force versus Experimental Drag Force.

from the linear nature of weight vs. time curve once CO_2 absorption was complete.

Fig.4.3 shows another sample recorder trace for absorption experiment (expt no. 8a) for 50 mole pct. Na_2O-20 mole pct. SiO_2-30 mole pct. B_2O_3 slag at 1000°C temperature. This fig. differs from Fig.4.1 in only one respect. The rate of weight loss due to volatilization is much larger as compared to that in Fig.4.1. However the nature of the curve as discussed earlier is the same.

Therefore the actual weight gain due to absorption of CO_2 could be determined only after correction of weight loss due to volatilization, according to the following equation.

$$\Delta W_c = \Delta W + R_v.t \qquad \ldots(4.1)$$

where ΔW = gain of weight (in mg.) as measured from the baseline after drag correction (discussed in Sec.4.2.2)..

R_v = Rate of volatilization under CO_2 gas, mg min^{-1} at

t = time from start of CO_2 flow, min.

and ΔW_c = corrected weight gain due to absorption of CO_2, mg.

R_v was determined from the slope of the linear weight loss region of the curve in flowing CO_2.

Fig.4.4 shows a few corrected weight gain (ΔW_c) vs. time plots in experiments with low rates of vaporization. It may be noted that the curves conform attainment of CO_2 saturation in slag well within the experimental time.

Fig.4.5 presents a few ΔW_c vs. time curves in

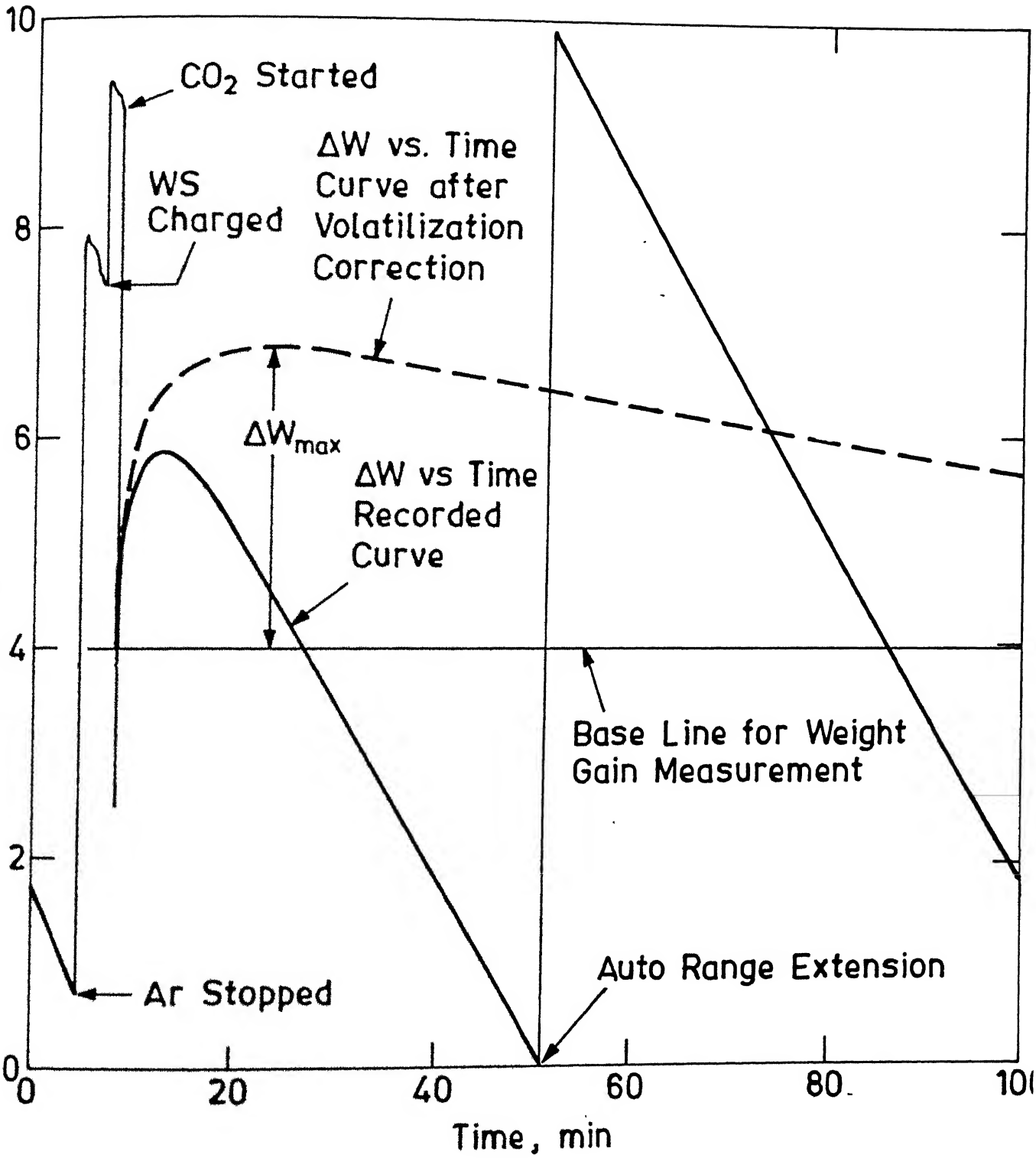

Fig. 4.3. Weight Gain versus Time Plot for 50 Na_2O - 20 SiO_2 - 30 B_2O_3 .

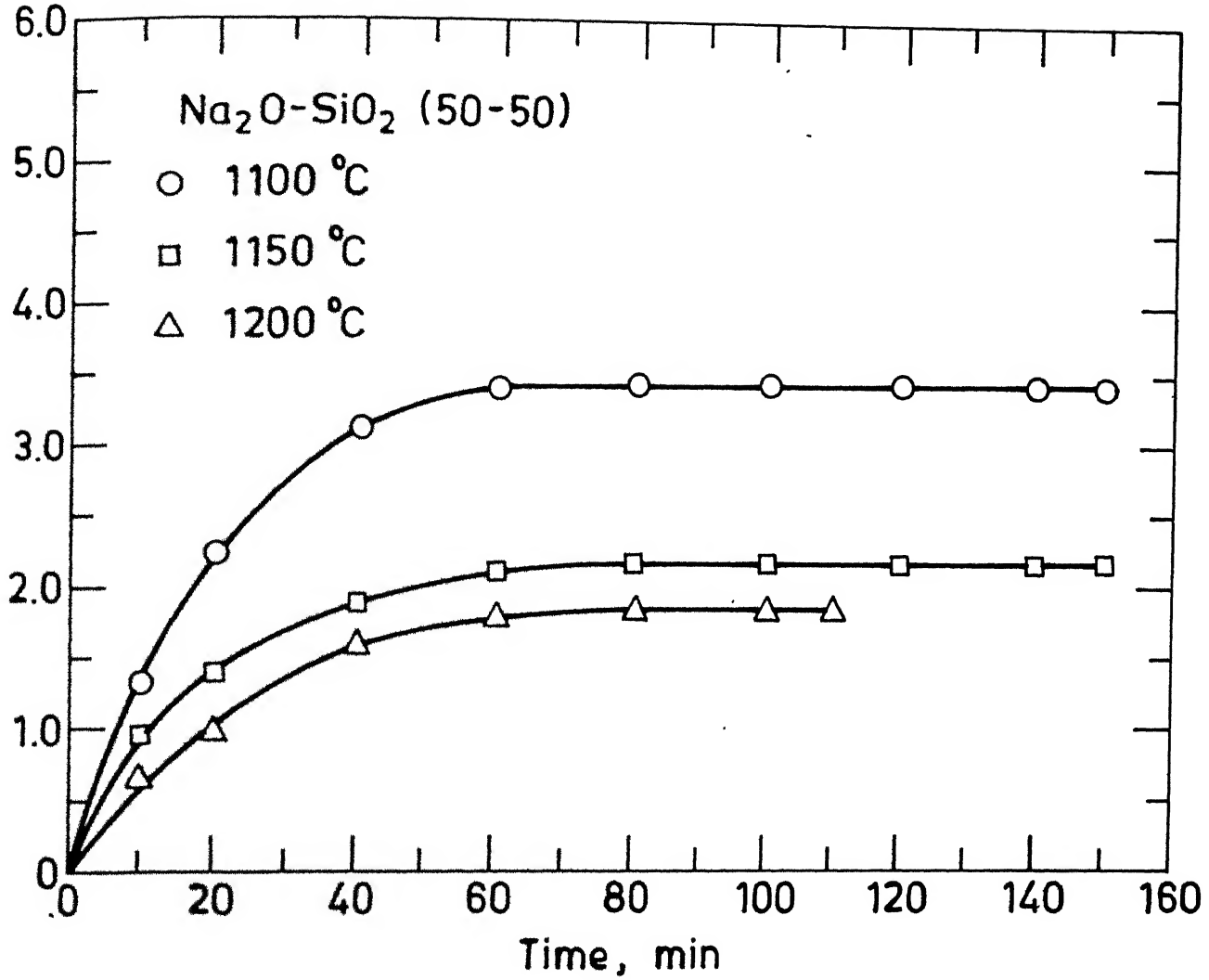

g. 4.4. Corrected Weight Gain versus Time Plots at Low Rates of Volatilization.

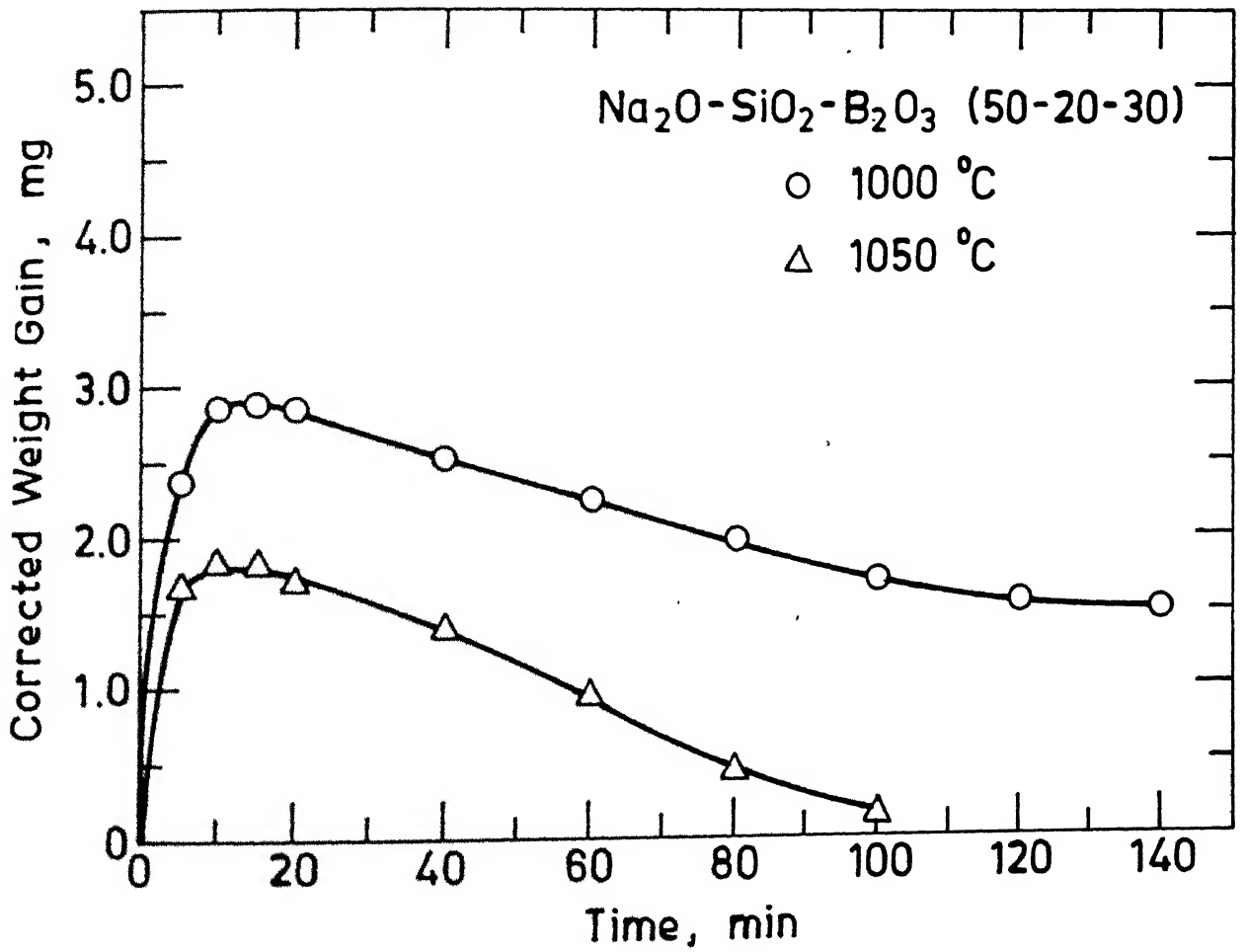

Fig. 4.5. Corrected Weight Gain versus Time Plots at High Rates of Volatilization.

experiments with high rates of volatilization. Here the curves exhibit maxima followed by a slow drooping tendency. This may be attributed to, first of all, a continuous decrease of slag weight, and secondly, change of slag composition due to preferential vapourization of Na_2O. Both these factors decrease amount of CO_2 absorbed in the slag and hence this drooping tendency. Therefore the solubility of CO_2 was determined from the maximum value of ΔW_c as shown in Fig.4.5.

Let $\Delta W_c = \Delta W_{max}$ and $t = t_s$ at the time, where values were taken for finding out solubility. Then ΔW_{max} gives the amount of CO_2 absorbed by the slag at saturation. Solubility of CO_2 in slag is given as $\Delta W_{max}/W_s \times 100$, in wt.pct., where W_s is weight of slag. Since there were changes in weight of slag as shown in Table 4.3, the value of W_s was taken at time t_s, by correcting the initial slag weight from recorder chart recordings. It may be noted that initial slag weight was determined before it was taken in the platinum crucible.

Table 4.3 compiles the data of successful experiments. It may be noted that there are some experiments carrying the same number but with a,b,etc. (for example Expts. 3a-3e). In these cases data were collected at one temperature, then temperature altered and again measurements were carried out on the same slag sample. Since it was the same slag sample the no. 3 was retained to indicate that. Table 4.3 also presents values of slag weight at saturation point, rate of volatilization in both Ar and in CO_2 gas. It also gives values of ΔW_{max} i.e. weight of CO_2 absorbed at saturation in time t_s as per the procedure already described.

Table 4.3 : Results of thermogravimetry experiments

Expt. No.	Slag composition, mole pct.			Temp. °C	Slag weight (W_s), gm		Rate of volatilization (R_v), mg min^{-1}		Quantity of CO_2 absorbed (ΔW_{max}), mg
	Na_2O	SiO_2	B_2O_3		Initial	at CO_2 saturation	In Ar	In CO_2	
1.	50	50	0	1100	0.4892	0.4928	0.008	0.01	5.12
2.	50	50	0	1250	0.5030	0.5002	0.025	0.015	1.60
3a.	50	50	0	1100	0.4016	0.4047	0.004	0.011	3.92
3b.				1150		0.4009	0.015	0.007	1.92
3c.				1200		0.3971	0.014	0.012	1.64
3d.				1250		0.3932	0.019	0.016	1.00
3e.				1100		0.3926	0.003	0.002	2.24
4a.	50	50	0	1100	0.4588	0.4614	0.003	0.002	3.44
4b.				1150		0.4562	0.012	0.007	2.16
4c.				1200		0.4517	0.013	0.013	1.84
4d.				1250		0.4471	0.020	0.015	1.04
5a.	50	0	50	1000	0.5979	0.5611	0.17	0.14	1.04
5b.				1050		0.5079	0.313	0.25	0.80
5c.				1100		0.4193	0.678	0.46	0.64
6a.	50	40	10	1000	0.4578	0.4618	0.001	0.026	6.00
6b.				1050		0.4480	0.068	0.046	4.28
7a.	50	30	20	1000	0.4224	0.4005	0.12	0.085	2.88
7b.				1050		0.3635	0.233	0.155	1.68
8a.	50	20	30	1000	0.6109	0.5942	0.206	0.153	2.88
8b.				1050		0.5280	0.360	0.264	1.84

Table 4.3 (Contd.)

Expt. No.	Slag composition, mole pct.			Temp. °C	Slag weight (W_s), gm		Rate of volatilization (R_v), mg min^{-1}		Quantity of CO_2 absorbed (ΔW_{max}), mg
	Na_2O	SiO_2	B_2O_3		Initial	at CO_2 saturation	In Ar	In CO_2	
9.	50	10	40	1000	0.5160	0.4919	0.173	0.118	1.76
10a.	60	0	40	1000	0.3949	0.3767	0.306	0.256	12.40
10b.				1050		0.2910	0.555	0.369	9.20
11.	50	40	10	1150	0.2983	0.2736	0.344	0.110	1.08
12a.	50	30	20	1000	0.5419	0.5310	0.104	0.072	3.68
12b.				1050		0.4993	0.212	0.146	2.32
12c.				1100		0.4509	0.443	0.200	1.92
13a.	50	40	10	1000	0.2949	0.2952	0.024	0.017	3.44
13b.				1050		0.2854	0.060	0.046	2.44

4.3 Discussions on Solubility of Carbon dioxide

4.3.1 Na_2O-SiO_2 (50:50) melt

Table 4.4 presents data on solubility of CO_2 in slags in wt. pct.. Reproducibilities were tested for the slag composition 50 Na_2O-50 SiO_2 at 4 temperatures, viz. 1100°C, 1150°C, 1200°C and 1250°C, as well as in a couple of Na_2O-SiO_2-B_2O_3 ternaries.

In Table 4.5, values of solubility for the different sets at same temperature and slag composition have been taken from Table 4.4 for the present investigation in order to discuss

Table 4.4 : Measured CO_2 solubility etc. of slags; also estimated optical basicity

Expt. No.	Slag composion, mole pct. Na_2O	SiO_2	B_2O_3	Temp. °C	CO_2 solubility, wt. pct.	Carbonate capacity (C_c)	Optical basicity (Λ)
1.	50	50	0	1100	1.04	1.42	0.76
2.	50	50	0	1250	0.32	0.44	
3a.	50	50	0	1100	0.97	1.32	
3b.				1150	0.48	0.66	
3c.				1200	0.41	0.56	
3d.				1250	0.25	0.34	
3e.				1100	0.57	0.78	
4a.	50	50	0	1100	0.75	1.02	
4b.				1150	0.47	0.64	
4c.				1200	0.41	0.56	
4d.				1250	0.24	0.33	
5a.	50	0	50	1000	0.19	0.26	0.65
5b.				1050	0.16	0.22	
5c.				1100	0.15	0.20	
6a.	50	40	10	1000	1.30	1.77	0.73
6b.				1050	0.96	1.31	
7a.	50	30	20	1000	0.72	0.98	0.71
7b.				1050	0.46	0.63	
8a.	50	20	30	1000	0.49	0.67	0.69
8b.				1050	0.35	0.48	

Table 4.4 (Contd.)

Expt. No.	Slag composion, mole pct. Na_2O	SiO_2	B_2O_3	Temp. °C	CO_2 solubility, wt. pct.	Carbonate capacity (C_c)	Optical basicity (Λ)
9.	50	10	40	1000	0.36	0.49	0.67
10a.	60	0	40	1000	3.29	4.49	0.72
10b.				1050	3.16	4.31	
11.	50	40	10	1150	0.40	0.55	
12a.	50	30	20	1000	0.70	0.95	
12b.				1050	0.46	0.63	
12c.				1100	0.42	0.57	
13a.	50	40	10	1000	1.17	1.60	
13b.				1050	0.79	1.08	

the issue of reproducibility of measurements more clearly. As may be noted from Table 4.5 that solubility values were fairly reproducible in most measurements, however in some there were more variations.

In Na_2O - SiO_2 melts several investigators have made measurements. Table 4.5 compares their values with those of the present investigation. For visualisation the values of solubility in 50 Na_2O - 50 SiO_2 composition have been plotted in Fig.4.6 at various temperature. So far as the present investigation is concerned, average values of the sets are also presented.

Table 4.5 : Comparison of CO_2 solubilities of present investigation with literature

Sr. No.	Slag composition, mole pct. Na_2O	SiO_2	B_2O_3	Temp. °C	CO_2 solubility, wt. pct. Present investigation	Average value	Literature (with references)
1.	50	50	0	1100	1.04, 0.97, 0.57*, 0.75	0.92	1.36[30], 1.19[27], 0.64[3]
				1150	0.48, 0.47	0.475	0.85[30]
				1200	0.41, 0.41,	0.41	0.49[30], 0.68[27], 0.18[3]
				1250	0.32, 0.25, 0.24,	0.27	0.13[30]
2.	50	40	10	1000	1.30, 1.17,	1.235	
				1050	0.96, 0.79,	0.875	
3.	50	30	20	1000	0.72, 0.70,	0.71	
				1050	0.46, 0.46,	0.46	

* Doubtful, hence not used for averaging

Table 4.5 also presents some values of CO_2 solubility from literature for Na_2O-SiO_2 melt. For Na_2O-B_2O_3, measurements of Pearce[35] are also available, however he has presented the data in such a way that extraction of reliable values are difficult and hence, has not been attempted. So far as sodium silicate is concerned it may be noted that there is considerable disagreement amongst the investigators. Values of the present investigation fall within the ranges reported in literature. It may be mentioned in passing that most of the investigators employed thermogravimetry technique except for Kawahara et al[29] and Pearce[34-35] who went for chemical analysis.

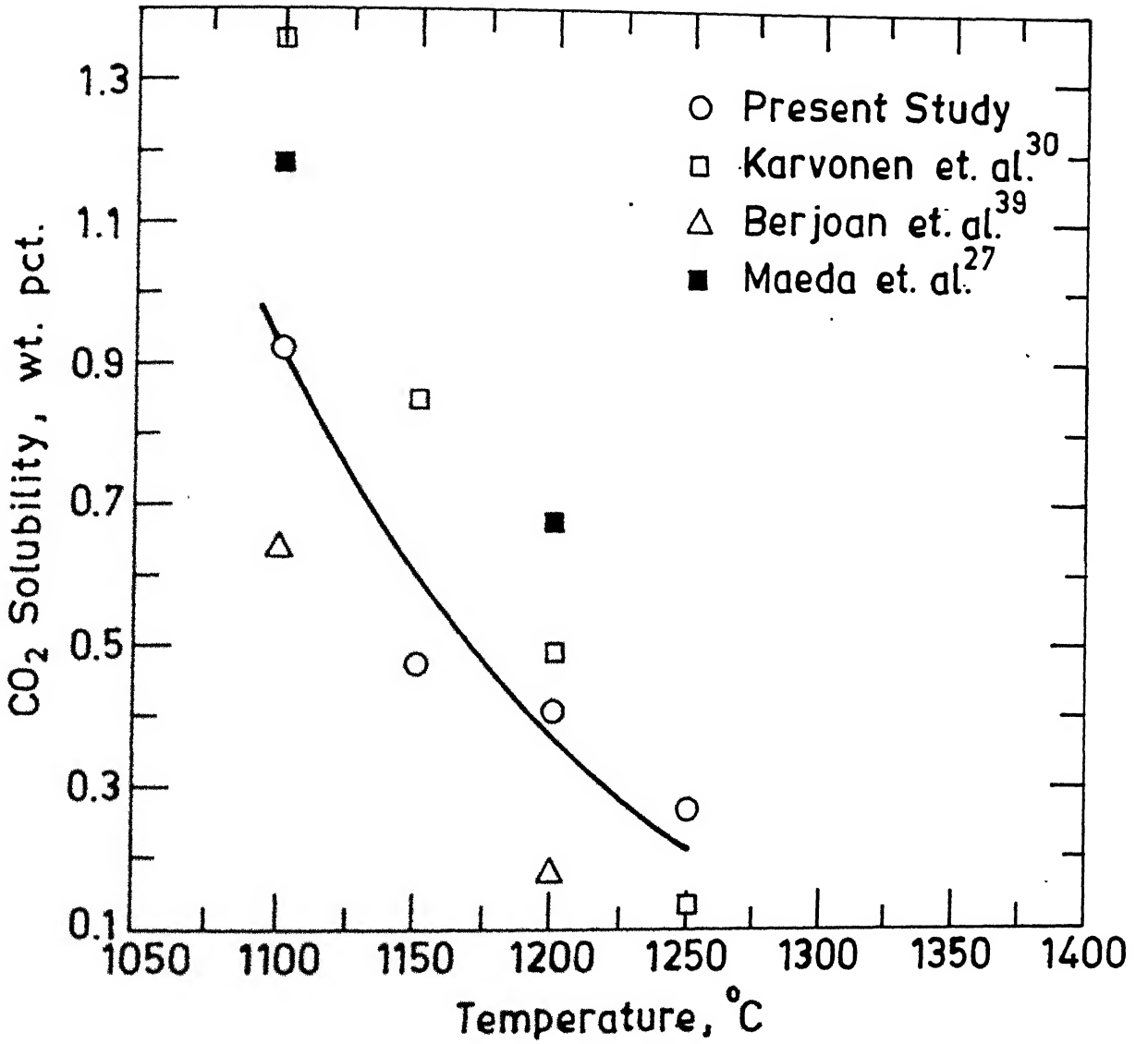

Fig. 4.6. A Comparison of Solubility Data for Carbon dioxide in $50Na_2O$-$50SiO_2$.

Fig.4.7 shows plots of ln(wt.pct.CO_2) as function of 1/T, where T is temperature in Kelvin for the present investigation. These have been fitted by straight lines by the method of least squares. Each line is for one slag composition. For the reaction

$$CO_2\ (g) = CO_2\ (slag) \qquad \ldots(4.2)$$

the excess partial molar free energy for the dissolution process may be expressed as

$$\bar{G}_{xs} = R\ T\ \ln \gamma_{CO_2(slag)} \qquad \ldots(4.3)$$

With a regular solution assumption,

$$\frac{\delta}{\delta\ (\frac{1}{T})}\ [\frac{\bar{G}_{xs}}{T}\ ] = \Delta\bar{H}_{CO_2} \qquad \ldots(4.4)$$

where $\Delta\bar{H}_{CO_2}$ is partial molar heat of mixing of CO_2 in slag. Thus from Eqs.(4.3) and (4.4)

$$\frac{\Delta\bar{H}_{CO_2}}{R} = \frac{\delta[\ln \gamma_{CO_2\ (slag)}]}{\delta\ (\frac{1}{T})} \qquad \ldots(4.5)$$

Again, $$\ln [\gamma_{CO_2(slag)}] = - \ln [\frac{X_{CO_2\ (slag)}}{P_{CO_2}}\ ] \qquad \ldots(4.6)$$

Since P_{CO_2} = 1 bar in all experiments,

From the above Equations,

$$\frac{\Delta\bar{H}_{CO_2}}{R} = - \frac{\delta(\ln X_{CO_2})}{\delta(\frac{1}{T})} = - \frac{\delta(\ln\ wt.pct.CO_2)}{\delta(\frac{1}{T})} \qquad \ldots(4.7)$$

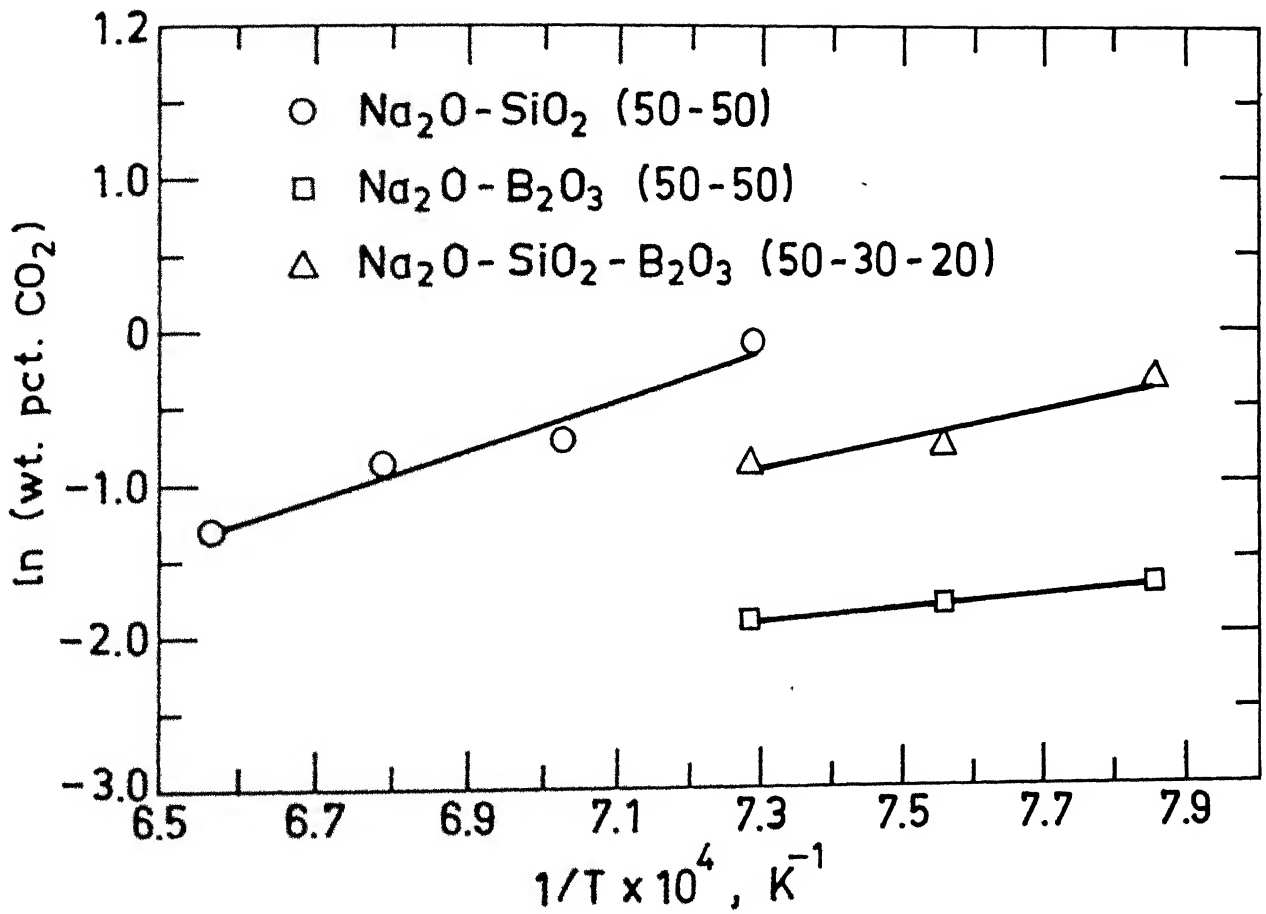

Fig. 4.7. Temperature Dependence of Carbon dioxide Solubility

Since solubility of CO_2 in slag is low, X_{CO_2} may be taken as proportional to wt. pct. CO_2 for the same slag composition.

From Eq.(4.7) and Fig.(4.7), therefore, $\frac{\Delta H_{CO_2}}{R}$ were found out from the slopes of least square fitted lines.

Slag composition	$\Delta \bar{H}_{CO_2}$, kJ mole^{-1}
Na_2O-SiO_2 (50-50)	- 133.52
Na_2O-SiO_2-B_2O_3 (50-30-20)	- 76.89
Na_2O-B_2O_3 (50-50)	- 34.54

Maeda et al[27] also determined $\Delta \bar{H}_{CO_2}$ for Na_2O-SiO_2 melts. For 50-50 composition they obtained a value of -131.67 KJ mole^{-1}. This compares well with the value in KJ mole^{-1} found in the present investigation. It may also be noted that $\Delta \bar{H}_{CO_2}$ becomes less negative as B_2O_3 replaces SiO_2 in the melt. This shows that the bond energy of CO_2 dissolved in melt is less for B_2O_3-containing melt as compared to SiO_2-containing melt. Of course this argument is strictly valid for regular solution.

4.3.2 Na_2O-B_2O_3-SiO_2 and Na_2O-B_2O_3 slags

It may be reiterated here that values of CO_2 solubility in literature on Na_2O-B_2O_3-SiO_2 ternary are not available. However some measurements were made in binary Na_2O-B_2O_3 melts by Pearce[35]. Unfortunately the author has presented his results in figures only and in such a way that it is difficult to extract values with reliability. Hence no comparison with his data is being attempted.

As Table 4.3 and 4.4 show that most of the compositions

for which data were available had $X_{SiO_2} + X_{B_2O_3} = 0.5$, where X denotes mole fraction. In order to ascertain how the solubility of CO_2 varied with increasing replacement of SiO_2 by B_2O_3, the solubilities at 1000°C and 1050°C have been plotted as function of $X_{B_2O_3} / (X_{B_2O_3} + X_{SiO_2})$ for the above melts in Fig.4.8. Therefore these curves correspond to melts with 50 mole pct. Na_2O.

Fig.4.8 shows that solubility of CO_2 decreases continuously with increasing B_2O_3 content in the melt, although mole pct. Na_2O was constant. It shows that the basicity, which may be related to activity of Na_2O in the melt, kept decreasing with increase in B_2O_3 at constant temperature. As expected the solubility went down with increase in temperature.

4.3.3 Correlation with optical basicity

Optical basicities of these melts were theoretically estimated following the procedure mentioned in chapter 2, section 2.4. The estimated values have been included in Table 4.4. Fig.4.9 shows that logarithm of carbonate capacities of Na_2O-B_2O_3-SiO_2 melts varied linearly with Λ at 1000°C, 1050°C and 1100°C. The linear regression fits yielded the following equations.

at 1000°C, $\log C_c = 9.59\ \Lambda - 6.785 \pm 0.032$ ...(4.3)

at 1050°C, $\log C_c = 8.80\ \Lambda - 6.39 \pm 0.037$ ...(4.4)

at 1100°C, $\log C_c = 7.28\ \Lambda - 5.42 \pm 0.009$ ...(4.5)

With reference to discussion in chapter 2, a linear dependence of $\log C_c$ with Λ is expected and the same has been found here for melts containing 50 mole pct.Na_2O. However the CO_2

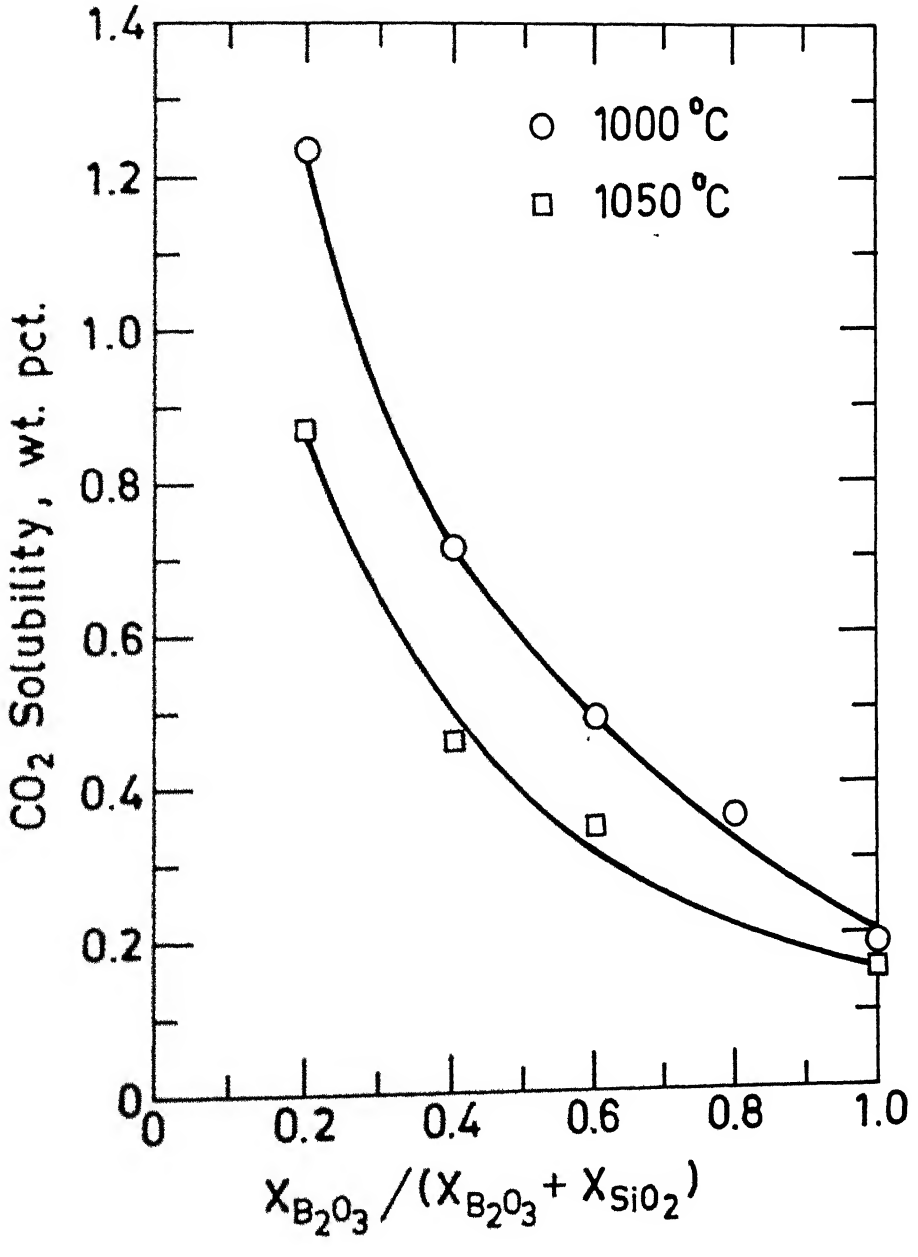

Fig. 4.8. Effect of B_2O_3 Addition to Na_2O-SiO_2 Melt on CO_2 Solubility.

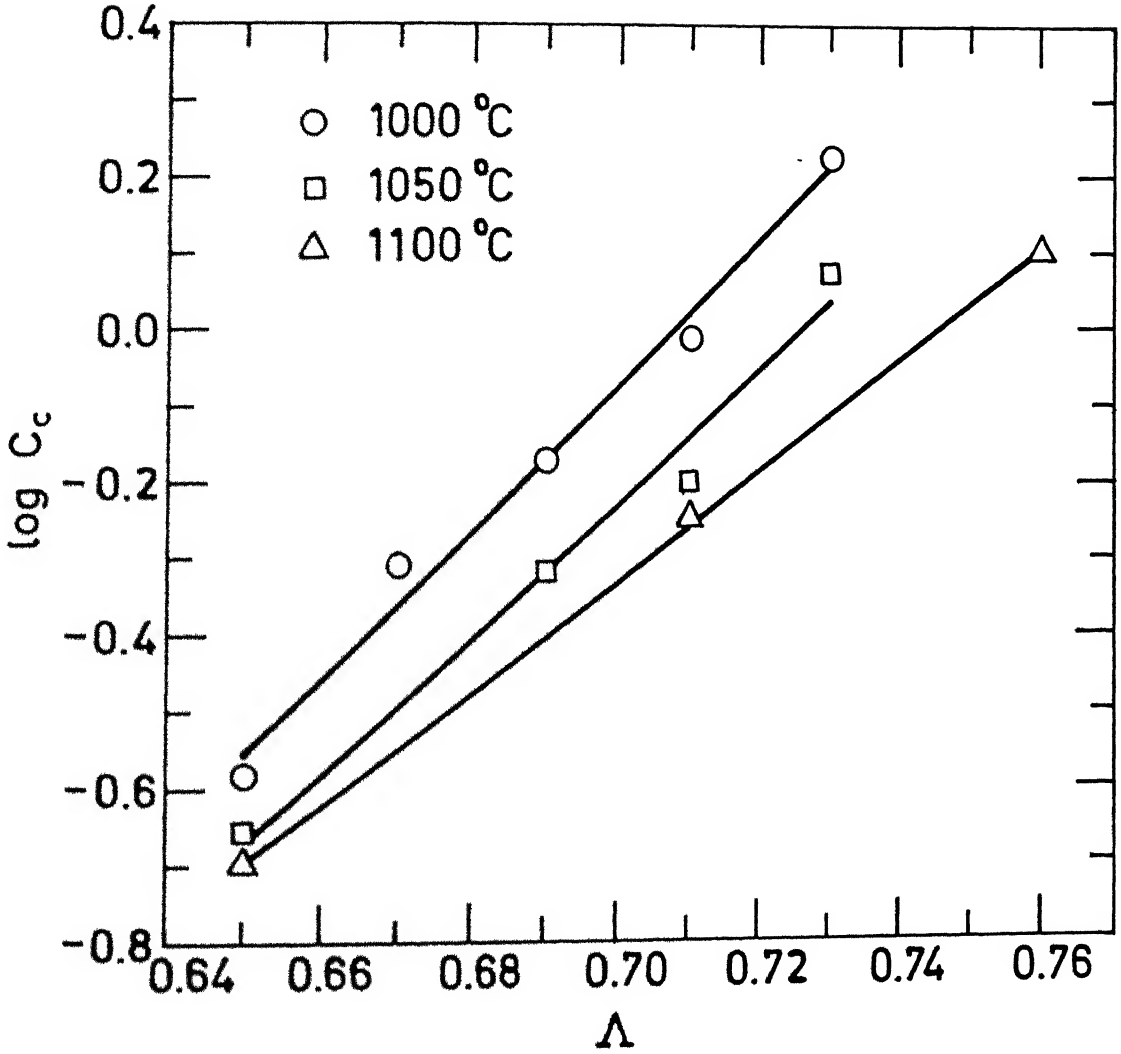

Fig. 4.9. Logarithm of Carbonate Capacity versus Optical Basicity of Slag.

solubility in 60 mole pct. Na_2O melt were much larger than the respective least square lines. Hence the latter was ignored for regression fitting. This behaviour pattern indicates that Λ is not a Universal measure of basicity. This logic is in conformity with conclusions drawn by some scientists (ch.2) that the optical basicity concept is to be employed with discretion.

4.4 Discussions on Volatilization

Table 4.3 presents values of rates of volatilization. An attempt would now be made to explain it. Table 4.6 shows vapour pressures of B_2O_3 as well as Na_2O as function of temperature. Vapour pressure of SiO_2 is very low, and hence is not included in the table.

Table 4.6 shows that the vapour pressure of B_2O_3 is much larger than that of Na_2O at the same temperature. Hence it is expected that vapourization rate in B_2O_3-containing melts would be much larger than those in Na_2O-SiO_2 melt. Fig.4.10 shows rate of volatilization in argon as function of $X_{B_2O_3}/(X_{SiO_2} + X_{B_2O_3})$ for 50 mole pct. Na_2O melts at 1000°C, 1050°C and 1100°C. Fig.4.10 confirms this expectation. The rate of volatilization increased significantly up to 30 mole pct. B_2O_3 with increasing B_2O_3 in the melt as well as increasing temperature. Above 30 mole pct. B_2O_3, the rate of volatilization decreases slowly. This nature of curve might be due to the decrease in activity of B_2O_3 in slag.

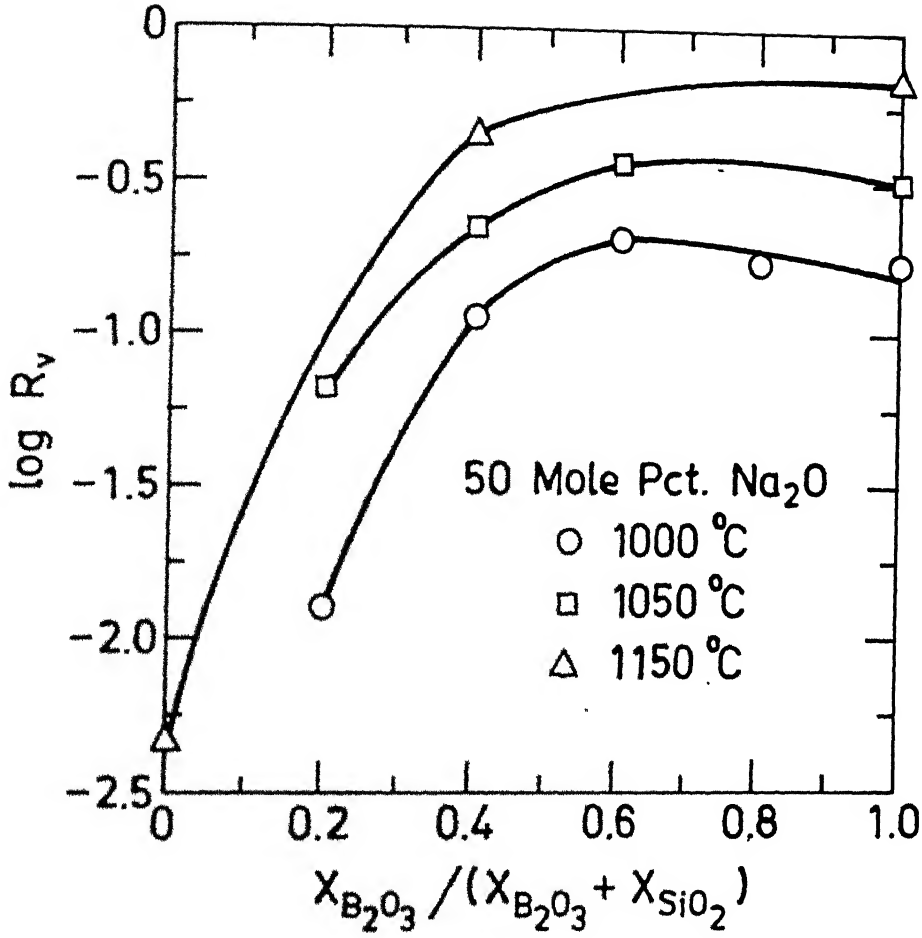

Fig. 4.10. Effect of B_2O_3 Addition on Sodium Silicate Melt on Rate of Volatilization in Argon.

Table 4.6 : Vapour pressures of Na_2O and B_2O_3 [40]

Oxide	Temperature (T), ^oK	Vapour pressure (P), atm.	Vapour pressure equation
Na_2O	800	4.84×10^{-22}	$\log P_{atm} = -24,044/T + 8.74$
	900	1.06×10^{-18}	
	1000	4.97×10^{-16}	
	1100	7.62×10^{-14}	
	1190	3.44×10^{-12}	
B_2O_3	1000	6.03×10^{-11}	$\log P_{atm} = -16,962/T + 6.742$
	1100	2.10×10^{-9}	
	1200	4.06×10^{-8}	
	1300	4.94×10^{-7}	
	1400	4.23×10^{-6}	
	1500	2.72×10^{-5}	

Assuming rate of vaporization to be controlled by mass transfer in the gas boundary layer, one can in principle calculate the mass transfer coefficient from the following equation.

$$\dot{n}_i = \frac{Ak_m}{RT} (p_i^e - p_i^o) \qquad ...(4.6)$$

where $\dot{n}_i$ = Molar rate of vaporization of a species i, gm.mole S^{-1}

A = Surface area of melt, m^2

K_m = Mass transfer coefficient, ms^{-1}

p_i^e = Equilibrium vapour pressure, atm.

p_i^o = Vapour pressure of species i in bulk gas (assumed to be zero)

$$p_i^e = p_i^e \text{ (pure i)} \times (a_i) \qquad \ldots(4.7)$$

where, a_i = Activity of species i in the melt.

Activity of B_2O_3 in these melts could not be located in literature. Activity of Na_2O in 50:50 Na_2O-SiO_2 melt at 1200°C is approximately 10^{-5}. However vapour pressure of Na_2O is available only up to its melting point, i.e. 917°C. Extrapolation using the vapour equation of Table 4.6 yielded a value of 3×10^{-7} atm. Using experimental data of vapourization rate and the above value of p_i^e, K_m was calculated with the help of Eq. (4.6). The value turned out to be approximately 10^5 m s^{-1}. This is absurdly large. No suitable explanation could be given for this discrepancy.

It may be mentioned in conclusion that the value of K_m would perhaps turn out to be approximately 10^2 m s^{-1}, since both vapour pressure as well as activity of B_2O_3 are orders of magnitude larger than those of Na_2O. Even the above value of K_m is much larger compared to that expected. However the existence of turbulence, vortex formation etc. in the gas on top of the melt may enhance K_m somewhat. This is just a guess. The main point is that the K_m value for vapourization of B_2O_3 is perhaps 10^3 times smaller as compared to that for Na_2O. Why it should happen this way is difficult to tell. It may be that impurities came into Na_2O-SiO_2 during slag making, which was behaving this way or it may be that the vapour pressure data of Na_2O is not reliable.

CHAPTER 5

SUMMARY AND CONCLUSIONS

1. The present study involved four steps:
   (a) choice of slag compositions,
   (b) preparation of slag,
   (c) measurement of CO_2 absorption at various temperatures and slag compositions
   (d) determination of solubility of CO_2 etc. from the above measurements.

2. Low melting slags based on B_2O_3 were chosen for measurement of CO_2 solubility. The slag (Na_2O-B_2O_3-SiO_2 and CaO-B_2O_3-SiO_2-CaF_2) were prepared from chemically pure Na_2CO_3, H_3BO_3, SiO_2, $CaCO_3$ and CaF_2. The B_2O_3 and CaO were obtained from calcination of H_3BO_3 and $CaCO_3$ respectively. Slags were melted in silicon carbide rod furnace at 1200°C under air in platinum or platinum-rhodium crucible. Na_2O-B_2O_3-SiO_2 slags had mostly 50 mole pct. Na_2O and varying B_2O_3 and SiO_2 content from 0 to 50 mole pct.

3. Measurement of CO_2 absorption was done on these polymeric melts in the temperature range of 1000-1250°C by thermogravimetric method using a Cahn 1000 recording balance.

4. The upward drag force on crucible due to gas flow and volatilization of components of slag affected the weight

gain. These were corrected for determination of actual weight gain due to absorption of CO_2 in slag.

5. Absorption of CO_2 was negligible for $CaO-B_2O_3-SiO_2$ slags. It was significant and measurable for $Na_2O-B_2O_3-SiO_2$ melts and the solubility values ranged between 0.15 and 3.29 wt.pct.

6. Reproducibility of CO_2 solubility values were tested. The values fell within the ranges reported in literature for 50 mole pct. Na_2O-50 mole pct. SiO_2 melt.

7. $\Delta\bar{H}_{CO_2}$ calculated for Na_2O-SiO_2 melt matched fairly with that of Maeda et al[27]. $\Delta\bar{H}_{CO_2}$ became less negative as B_2O_3 replaced SiO_2 in the melt. This shows that the bond energy of CO_2 dissolved in melt is less for B_2O_3-containing melt as compared to SiO_2-containing melt. Of course this argument is strictly valid for regular solution only.

8. The solubility of CO_2 decreased continuously with increasing B_2O_3 content in the melt, although mole pct. Na_2O was constant at 50. It shows that the basicity decreases with increase in B_2O_3 at constant temperature at 50 mole pct. Na_2O. As expected, solubility went down with increase in temperature.

9. For melts containing 50 mole pct. Na_2O, a linear dependence of log C_c with optical basicity of slag was found, as expected. However, the CO_2 solubility in 60 mole pct. Na_2O was much larger and did not fit with the least

square line. This behaviour pattern indicates that Λ is not a Universal measure of basicity, and is to be used with discretion.

10. With increasing B_2O_3 content in the melt, the rate of volatilization increased significantly up to 30 mole pct. B_2O_3, beyond which the rate of volatilization decreased slowly. The increase can be explained by higher vapour pressure as well as activity of B_2O_3.

11. In Na_2O-SiO_2 (50:50) melt, the mass transfer coefficient for volatilization of Na_2O at 1200^{o}C was found to be approximately 10^5 m s^{-1}, which is absurdly large. No suitable explanation could be given for this discrepancy. However for B_2O_3 volatilization value of k_m may be of the order of 10^2.

CHAPTER 6

SUGGESTIONS FOR FUTURE WORK

The present investigation has been carried out to measure the carbonate capacity of Na_2O-B_2O_3-SiO_2 melts at different temperatures. Here thermogravimetric method has been employed. As an extension of this work in future, it would be worth studying the following aspects :

1. The effect of addition of CaO and CaF_2 in the above melts on carbonate capacity,
2. Calculation of $\Delta\bar{H}_{CO_2}$ for above ternary melts, by performing the CO_2 solubility experiments at more than 4 temperature, for same slag compositions,
3. Measurements of activities of B_2O_3 and Na_2O,
4. Measurements of sulphide and phosphate capacity of these melts and correlation with carbonate capacity.

REFERENCES

1. A. Ghosh and H.S. Ray; Principles of Extractive Metallurgy, The Indian Institute of Metals, Calcutta, India (1983).
2. R.G. Ward; An Introduction to the Physical Chemistry of Iron and Steel Making, Edward Arnold Publishers Ltd., London (1962).
3. F.D. Richardson and C.J.B. Fincham; Proceedings of the Royal society (London), A (1954), 223, p.40.
4. K. Susaki, M. Meada and N. Sano; Met. Trans. B, 21B (February 1990), p.121.
5. R.G. Reddy and M. Blender; Met. Trans., 18B (September 1987), p.591.
6. Carl Wagner; Met. Trans., 6B (September 1975), p.405.
7. N. Sano; in the Elliott Symposium Proceedings, ISS, Cambridge, MA, USA (1990), p.163.
8. D.J. Min and R.J. Fruehn; Met. Trans. B, 21B (1990), p.1025.
9. E. Martinez R. and N. Sano; Met. Trans. B, 21B (1990), p.97.
10. K. Tomioka and H. Suito; Steel Research (1992), p.1.
11. A. Muan and E.F. Osborn; Phase Equilibria Among Oxides in Steelmaking, Addison Wesley Publishing Company Reading Mass (1965).
12. J.A. Duffy and M.D. Ingram; J. of Noncryst. Solids, 21 (1976), p.373.
13. J.A. Duffy and M.D. Ingram; J. of Inorg. and Nuclear Chem., [illegible] p.1203

14. C.L. Carey, R.J. Serje, K. Gregory and He Qinglin; 3rd Int. Conf. on Molten Slags and Fluxes, (27-29 June,1988), p.157.

15. J.A. Duffy; in ref. 14, p.154.

16. J.A. Duffy; Iron Making and Steel Making, **17** (1990), No.6, p.410.

17. J.A. Duffy, M.D. Ingrom, J.D. Sommerville; J. Chem. Soc., Faraday Trans., **74** (1978), p.1410.

18. T. Nakamura et al; J. Jpn Inst. of Metals **50** (1986), p.456.

19. D.R. Gaskell; Met. Trans. B, **20B** (February 1989), p.113.

20. A. Bergman and A. Gustafsson; in ref. 14, p.150.

21. D.J. Sosinsky and I.D. Sommerville; Met. Trans. B, **17B** (1986), p.331.

22. R.G. Reddy, M. Blander; Met. Trans., **18B** (1987), p.591.

23. T. Mori; Trans. Jpn. Inst. Met., **25** (1984), p.761.

24. I.D. Sommerville and D.J. Sosinsky; Proc. Second Int. Symposium on Metall. Slags and Fluxes, TMS-AIME (1984), p.1015.

25. M.D. Ingram; in ref. 14, p.166.

26. T. Yokokawa and T. Maekawa; in ref.14, p.313.

27. M. Maeda, A. McLean, H. Kuwatori and N. Sano; Met. Trans. B, **16B** (September 1985), p.561.

28. D.J. Sosinsky, I.D. Sommerville and A. McLean; 5th I.I.S. Congress, Process Tech. Proc., 6, Washigton, DC, ISS (1986), p.697.

29. T. Kawahara, K. Yamagata and N. Sano; Steel research, **57** (1986), No.4, p.160.

30. P. Kuparinen, H. Tonteri and L.E.K. Holappa; Scand. Journal

Metallurgy, **17** (1988), p.151.

. T. Ikeda and M. Maeda; Proceedings of Sixth International Iron and Steel Congress (1990), Nagoya, ISIJ, p.272.

. M. Maeda and T. Ikeda; in ref. 14, p.107.

. T. Kawahara, S. Shibata and N. Sano; in ref. 28, p.691.

. M.L. Pearce; Journal of the American Ceramic Soc., **47**, No.7 (July 1964), p.343.

. M.L. Pearce; Journal of the American Ceramic Soc., **48**, No.4 (April 1965), p.175.

). B.K. Goswami; Elements of Inorganic Chemistry, part I, Moulik Library Calcutta.

'. A. Ghosh; Proc. Workshop on Role of Reductants in Sponge Ironmaking, Ranchi (1983), p.25.

3. V.D. Eisenhuttenleute; Slag Atlas, Prepared by the Committee for Fundamental Metallurgy (1981).

). R. Berjoan and J.P. Coutures; Rev. Int. Hautes Refract Fr 20 (19[illegible]), p.115.

0. J.F. Elliott and M. Gleiser; Thermochemistry for Steelmaking, Vol. 1, Addison-Weseley Publishing Company, Inc., (1960).

APPENDIX

Drag Calculation

Drag force is calculated from the following relation :

$$F_K = A\ K\ f \qquad \text{(A1)}$$

where A = projected area of crucible perpendicular to flow of gas

K = characteristic kinetic energy per unit volume of the gas

f = drag-coefficient

Assuming crucible as spherical body, then

$A = \frac{\pi}{4} d^2$, where d = diameter of crucible, cm

$K = \frac{1}{2} \rho u_0^2$, where ρ = density of gas, gm cm^{-3} and u_0 = speed of gas, cm s^{-1}

Then

$$F_K = \left(\frac{\pi}{4} d^2\right)\left(\frac{1}{2} \rho u_0^2\right) f$$

$$= \frac{\pi}{8} d^2 \rho u_0^2 f \qquad \text{...(A2}$$

In present study, d = 1 cm.

$$u_o = \frac{\text{gas flow rate } (cm^3\ s^{-1} \text{STP}) \times \frac{T}{273}}{\frac{\pi}{4} \times (\text{inner diameter of furnace tube}, cm^2)}$$

Let gas flow rate is Q $cm^3\ s^{-1}$ (STP), then

$$u_0 = \frac{Q \times T}{273 \times \frac{\pi}{4} (1.7)^2} \ cm\ s^{-1}$$

$$= 1.61 \times 10^{-3}\ Q\ T \ cm\ s^{-1} \qquad \text{...(A3)}$$

$$\rho_{Ar} = \frac{39}{22400} \times \frac{273}{T} = \frac{0.475}{T} \text{ gm cm}^{-3}$$ then from Eq. (A2) and (A3),

$$F_k = \frac{\pi}{8} \times 1^2 \times \frac{0.475}{T} \times (1.61 \times 10^{-3}\ QT)^2\ f$$

$$= 4.84 \times 10^{-7}\ Q^2\ T\ f \qquad \ldots(A4)$$

$$\text{Reynolds No.} = Re = \frac{d\ u_0\ \rho}{\mu} \qquad \ldots(A5)$$

where μ = viscosity of gas, poise

Since, $$\mu_{Ar} = 13.15 \times 10^{-6}\ T^{1/2} \text{ poise}$$

$$Re = \frac{1 \times (1.61 \times 10^3\ Q\ T) \times \frac{0.475}{T}}{13.15 \times 10^{-6}\ T^{1/2}}$$

$$= 58.16\ Q\ T^{-1/2}$$

From f vs. Re relationship for flow around sphere,

$$f = \frac{18.5}{Re^{375}} = \frac{18.15}{(58.16\ Q\ T^{-1/2})^{0.6}}$$

$$= 1.59\ Q^{-0.6}\ T^{0.3} \qquad \ldots(A5)$$

then from Eq. (A4) and (A5), we get

$$F_k = 4.84 \times 10^{-7} \times 1.59\ Q^{1.4}\ T^{1.3}$$

$$= 7.7 \times 10^{-7}\ Q^{1.4}\ T^{1.3} \text{ gm cm s}^{-2} \qquad \ldots(A6)$$

or, $$F_k = 7.85 \times 10^{-7}\ Q^{1.4}\ T^{1.3} \text{ mg wt.} \qquad \ldots(A7)$$

Example At $Q = \frac{200}{60}\ cm^3\ s^{-1}$ and $T = 1273$ K

$$F_k = 7.85 \times 10^{-7} \times \left(\frac{200}{60}\right)^{1.4} (1273)^{1.3}$$

$$= 4.6 \times 10^{-2} \text{ mg wt.}$$

ME-1992-M-SIN-MEA